

EXAMPLES' DESCRIPTION

Contents

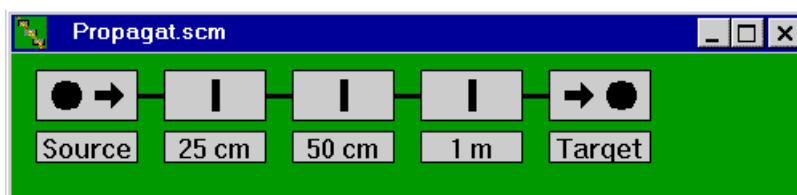
EXAMPLES FOR DEMO	5
Example 01. Propagation.....	5
Example 02. Diffraction.....	6
Example 03. Magnification (Fast Fourier Interpolation)	9
Example 04. Diffraction of an Elliptical Beam	10
Example 05. Obscuration.....	11
EXAMPLES FOR BASIC	13
Example 10. Spatial Frequency Filtering	13
Example 11. Zernike Phase Contrast Visualization Method.....	14
Example 12. Interplay of Diffraction and Gain Saturation.....	15
PRIMARY SEIDEL ABERRATIONS	16
Example 20. Spherical Aberration: Beam Focusability.....	18
Example 21. Spherical Aberration: Beam Quality.....	20
Example 22. Astigmatism	21
Example 23. Astigmatism: Modeling of Cylindrical Lenses.	22
TELESCOPES	23
Example 30. Beam Expander: Imaging by Keplerian and Galilean Expanders.....	23
Example 31. Beam Expander: Spherical Aberrations and Beam Quality	24
BEAM TRANSFORMS	25
EXAMPLE 40. Beam Shift: Accuracy, Simulation Noise	26
EXAMPLE 41. Beam Shift: Acceptable values.	27
EXAMPLE 42. Beam Rotation: Accuracy, Simulation Noise	28
EXAMPLE 43. Beam Rotation: Errors caused by abrupt boundary	29
EXAMPLE 44. Beam Rotation: Arbitrary Center of Turn	30
EXAMPLE 45. Beam Reflection: Two Reflections equal Rotation	31
OBSTACLES II	32
EXAMPLE 60. Obscuration: Three Small Specks, Spatial Filtering	33
EXAMPLES 61 and 62. Obscuration: Babinet's principle.....	34
EXAMPLE 63. Obscuration: Pinhole size optimization.....	35
EXAMPLE 64. Dusty surface (Dust): Noise - intensity fluctuation.....	37
EXAMPLE 65. Dust: Far field diffraction.....	38
EXAMPLE 66. Dust: Spatial filtering of intensity noise	39

EXAMPLES FOR DEMO

Choose **File / Open** Scheme. FRESNEL displays the Open File dialog box. Specify the file for scheme you like to open, e.g., **EXM 01-Propagat.scm**. Press **OK** or **Enter**.

Example 01. Propagation

The Scheme Window appears. In the case of **EXM 01-Propagat.scm** it contains Source, Target, and three View screens.

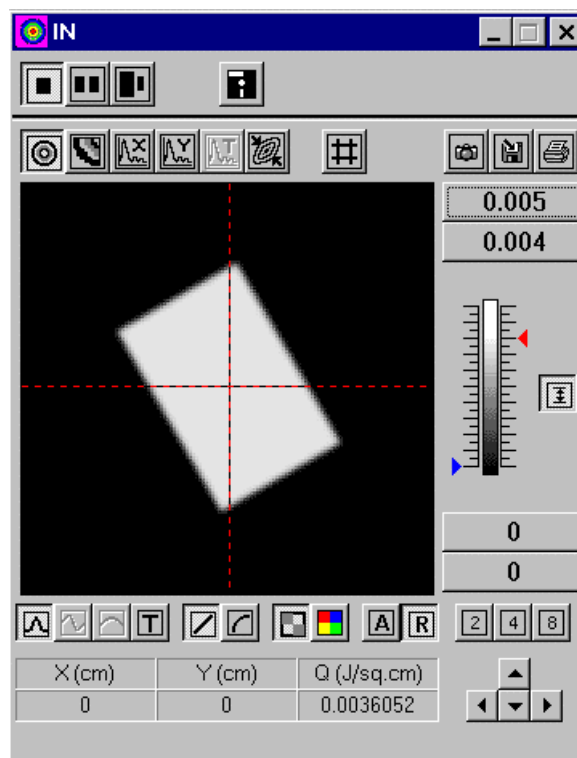


In **EXM 01-Propagat.scm** each View screen has a label indicating the distance from the Source. All elements are sitting on a connecting line.

To open an element dialog box just double click its pictogram with a mouse. If you do this with View screens of our **EXM 01-Propagat.scm**, you will see real distances between previous and current elements (respectively 25, 25, and 50 cm). You will also notice that the function "pause" is on. It means that when the beam hits the View screen, the propagation calculations stop until the next **Run** command.

You can also double click the Target. You will see in this case that the Target distance is 900 cm from the previous View screen, thus the total distance between Source and Target is 10 m. You will notice also that the Magnification is 1.

Now you can double click the Source. You will see the list of Input Beam Shapes.



You can choose any, but here you need file **EXM 01-Propagat.pls**. So choose **Load from file | EXM 01-Propagat.pls** and in the "In" Beam Window you will get a beam of predefined type: flat-topped rectangular beam of 0.44 by 0.66 cm given on a scale 1.28 cm (with pixels number 128x128), rotated by 30°. The beam wavelength is 530 nm and the energy is 1 mJ. The softening scale (see Help for this term) is 0.015 cm. (As soon as **EXM 01-Propagat.pls** is of the predefined type its parameters may be checked by double clicking Source again and choosing Flat-topped beam. Try this and return back pressing Cancel.)

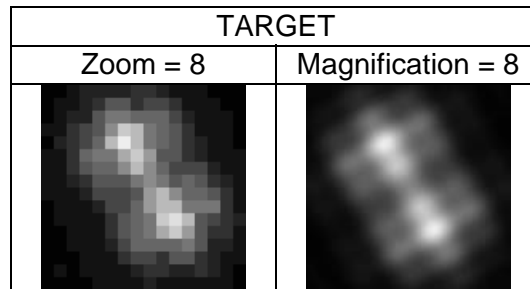
Now you are ready to run the scheme. Choose **Run** or corresponding button on the Main FRESNEL Toolbar.

The calculations start and in a second, the Current Beam Window will appear. The picture will change after passing prescribed distance to the next element. When the calculation discretization is small and your computer is fast enough, you will not be able to follow all the beam changes. Thus before or after an element you can arrange pauses or checkpoints (as we did in **EXM 01-Propagat.scm**). Using buttons in the Beam Window you can examine beam distributions on a linear or logarithmic scale, take profiles along X- and Y-axes, observe temporal shape changes and so forth. Pressing **Run** again, you will proceed to the next element. The color of the passed element turns green.

FRESNEL uses "Automatic Scale Adjustment Procedure" to minimize the aliasing effect. Therefore, if you propagate the beam "too far" it can occupy only a small portion of the Beam Window pane (as it is at the Target in **EXM 01-Propagat.scm**).

You may apply Zoom = 8 and press the button  that will display zoom area, but this will not result in getting more information, just the number of pixels displayed will be 64 times less.

DO NOT WORRY! THE RESOLUTION COULD BE IMPROVED! However, you will have to edit the Target parameters. Choose Magnification=8 and pause - "on". Restart calculations from the very beginning. Now after finishing all calculation steps, in front of the Target you will see small size beam again, but pressing Run for the last time, you trigger the Magnification 8* procedure. After finishing it (Target color will turn green) you will have much more detailed picture than it was in the case when Zoom = 8 was used. Now the number of the pixels in the image is 128x128 again. Just compare.



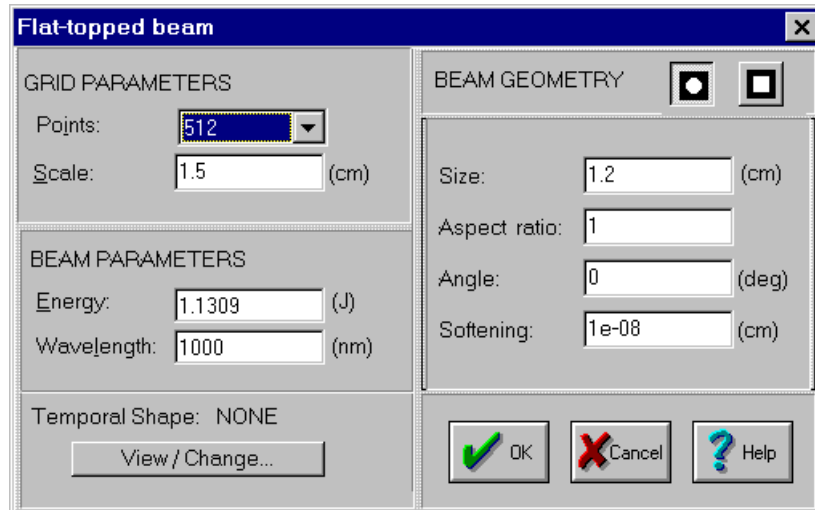
The pictures above exhibit pronounced diffraction of the beam.

More detailed study you can perform for the diffraction onto the sharp edge diaphragm. It is a "touchstone" for numerical calculations in optics.

Example 02. Diffraction

Load **EXM 02-Diffract.scm** and respective input beam given in **EXM 02-Diffract.pls**. You can see distribution parameters if you double click "Source" and choose "Flat-topped beam". It is a circular beam of the diameter $2w = 1.2$ cm, and of 1000 nm wavelength. Its energy has been chosen to correspond to the flux of 1 J/cm^2 . The circle diameter ratio to the calculation grid scale ($L_0 = 1.5$ cm) is 0.8 that provides most accurate result for plane wave diffraction. Do not believe when somebody claims that it is necessary to stipulate large guard zone around the beam (i.e. choose $L_0 \gg 2w$) to avoid the aliasing. It is much better to use the correct calculation procedure instead. In FRESNEL this is done automatically for a beam

propagating in free space or through any centered sequence of convergent or divergent lenses.



In order to study beam propagation, several distances were chosen that correspond to different Fresnel numbers $N_f = w^2/(\lambda \cdot Z)$: $N_f = 6$ at $Z = 6\text{m}$; $N_f = 5$ at $Z = 7.2\text{m}$; $N_f = 4$ at $Z = 9\text{m}$ (Target). We remind that the distance to first element is measured starting from Source, while for each of the following it corresponds to the distance from a previous element. Looking through the dialog boxes of the elements used in this scheme one can see these distances. Run the program and when it stops after $N_f = 6$ you will see the beam as a small light spot inside the black square of the calculation grid.

Do not be surprised! Pressing the  button below the beam image, you will see that the full scale of the calculation grid is 20.48 cm (the step of sampling points 0.04 cm). The program has chosen such a scale automatically in order to minimize calculation errors. Pressing the energy density button , you will return to a 2D picture of the beam. We recommend now to press  and to use two-pane Beam Window. If you did so, first, press X-profile button  in the left pane, and then press Zoom button . The image size is now OK, but the resolution seems to be not sufficient.

Do not hurry in making conclusion. Wait a little bit. Recall several facts that the theory gives for the near field ($N_f > 1$) diffraction onto a circular diaphragm. The number of main maxima in a cross section should be equal to the Fresnel number (N_f) and energy density at $r = 0$ should be equal to null for even N_f . In our case it is $\approx 4.6 \cdot 10^{-6} \text{ J/cm}^2$ that compared with 1 J/cm^2 for the initial beam gives not bad calculation accuracy. Our next stop is at odd $N_f = 5$ and the theory predicts the energy density 4 times higher than the initial one at $r = 0$. Leave the Beam Window settings unchanged, and then on the next stop, you will see, as it is now, only a central part of the calculated field. If you like, switch off Zoom to observe full image.

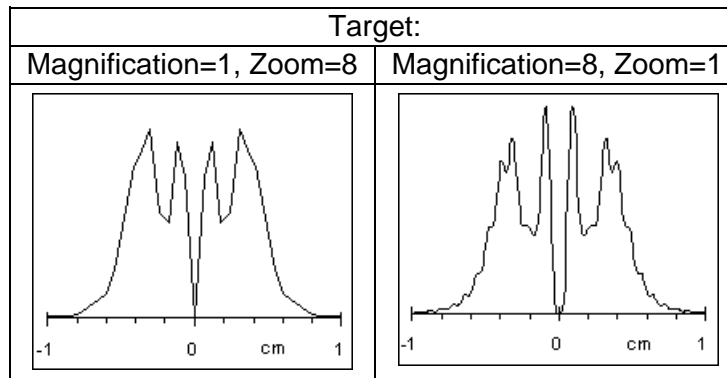
Press **Run** and continue the calculations. In a moment you will get the 2D picture and the plot for the distance 7.2 m ($N_f = 5$). As it should be, the energy density at $r = 0$ is four times higher than the initial one (with the accuracy 10^{-4}), and the number of the main maxima is 5.

Press **Run** again. After calculations you will stop at $Z = 9\text{m}$ ($N_f = 4$) just before the Target. Do not hurry, please. As we could suspect the energy density for $r = 0$ is very low again. As it was before the spatial resolution is not sufficient to observe the picture in details. As soon as the information concerning the complex electric field is quite sufficient (as for our previous stops at $N_f = 6$ and 5) we can reconstruct the energy density distribution with much better spatial resolution. Before we proceed save current beam distribution as *temp1.pls* by pressing **Save** button  in the Beam Window.

Next, switch off Zoom and check the parameters set for the Target. You will see that Magnification is equal to 8, as it has been chosen beforehand. This very operation will be

performed if you press **Run**. After the procedure of the 2D Fourier interpolation, you can observe the calculation result with 8 times higher resolution both in the plot and in the 2D distribution.

It is worth to compare the output picture with that we have had before magnification. To do this load *temp1.pls* as input beam. Switching on Zoom = 8 you will get for the latter picture the same scale (3.84 cm) as for the output beam. Obviously, the image after the magnification (see their profiles in the figure below) contains more details indistinguishable without this procedure. How precise is the procedure itself, we shall discuss in successive examples.



Those who want to evaluate the accuracy of the calculations in *EXM 02-Diffract.scm* is invited to load *EXM 02-Diffract.pls* again. After this press an options button on the Scheme toolbar and change the "precision" check level to 0.001. Now if you run the scheme, on some steps of calculations you will see Precision warning. Answer each time Yes. The value of the current precision indicates that within the calculated field at least one point has the accuracy of the order of that is shown. Usually, it is worthless to hope that after performing complete calculations (propagation through a series of optical elements) the accuracy is essentially better than maximum value of the current precision evaluated when calculations are in progress. However, there are exceptions. Total accuracy can be sometimes better sometimes worse than indicated. I.e. the current precision value serves just to give an approximate estimation of the accuracy. Nevertheless, in above example of *EXM 02-Diffract.scm* the current precision value corresponds to the calculation accuracy very well. It has been checked by direct calculations of the Fresnel-Kirchhoff integral. Thus, all beam distributions are quite adequate to real diffraction on the circular sharp edge diaphragm with the accuracy of about $2\div 5 \times 10^{-3}$.

If you wish, you can now modify the *EXM 02-Diffract.scm* or create a new one. When creating a new scheme you will need to load the input beam *EXM 02-Diffract.pls* distribution, arrange propagation distance/distances, and choose Magnification value on a Target. In the case of *EXM 02-Diffract.pls* it is recommended to use the following *Magnification* values depending on the distance between the Source and the Target.

Z, m	1-2	2-4	4-8	8 and more
Magnif.	2	4	8	16

Usually to observe the distribution with sufficient resolution it is quite enough to have the Magnification = 8.

Presented example was chosen to demonstrate that:

- Program FRESNEL automatically adjusts the calculation scale in order to provide the highest possible accuracy.
- User has no need in deciding which propagation method should be applied in each particular case as it is should be done often in other programs.

Above two advantages are very noticeable (in FRESNEL Pro version) when the

propagation and diffraction are studied for a complex system of lenses and other optical elements with the arbitrary distances between them.

Program FRESNEL performs the evaluation of the calculation precision for each step of the propagation indicating the degree of confidence to the obtained result.

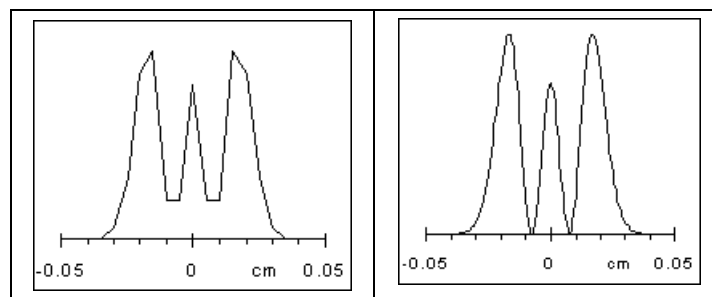
The Magnification procedure permits to analyze results with required spatial resolution.

The same procedure is applied automatically when the radiation passes through the apertures of the optical elements. In many cases, this results in the essential enhancement of the calculations accuracy.

Example 03. Magnification (Fast Fourier Interpolation)

Open **new** scheme and load the input radiation from the file *EXM 03-Magnif.pls*. It is a $TEM_{2,0}$ mode of rectangular symmetry and its parameters can be seen if you return back to selecting Input beam shape and choose Resonator mode. You will see: Scale $L_0 = 1.28$ cm, discretization $N = 256$, beam size $w = 0.015$ cm, wavelength 1000 nm.

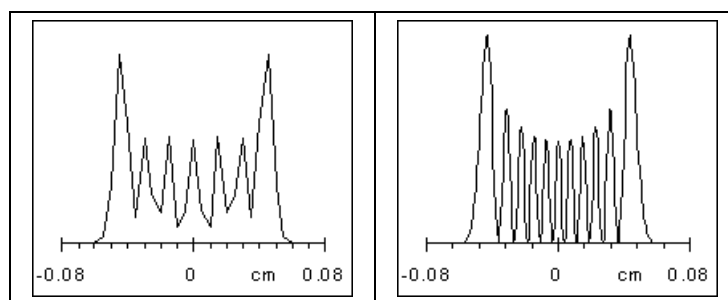
Now, double click Target, switch pause "off" and set the Magnification = 8.



Running the scheme produces the 8* magnification (right profile in the figure above) of the initial beam that can be compared with 8* zoomed profile of the initial beam (left profile).

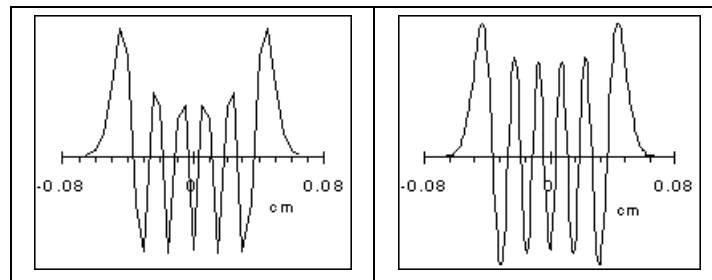
Exporting the profile of the beam into Excel or other program one can compare magnification result with analytical data for $TEM_{2,0}$ mode.

User can now change first TEM mode index of the input radiation from 2 to 10. After running the scheme two X-profiles for the $TEM_{10,0}$ beam, obtained at Zoom = 8 and Magnification = 8 can be obtained for $TEM_{10,0}$ mode as shown in the next picture.



One can see that zoomed beam exhibits only 7 maxima while the magnified beam has 11 maxima as it should be for the mode $TEM_{10,0}$.

Setting Magnification = 1 and running the scheme again one can now press the "amplitude" button to restore the $TEM_{10,0}$ mode amplitude distribution. The X-profiles for both zoomed and magnified beam amplitudes do exhibit 11 extremums, as it should be. These profiles are presented below.



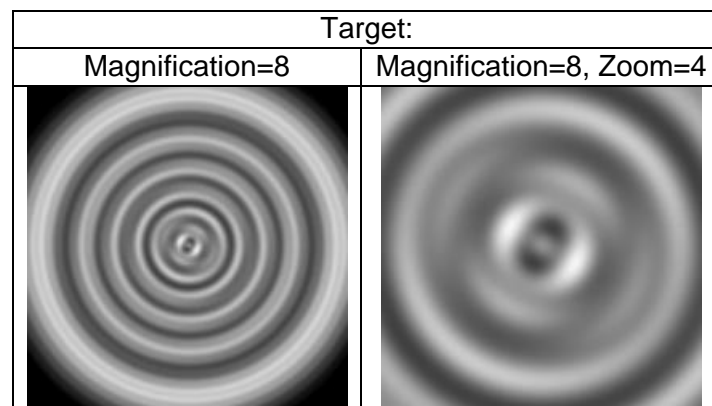
Therefore, there is no miracle that the Fourier interpolation restores beam shape quite correctly: the field is defined by its amplitude and phase rather than by the energy density distribution.

It is recommended now to change the TEM mode index of the input radiation to 20. The test, which in fact describes the propagation of the beam to the far field zone, shows that the expected precision of the calculations with this beam is very poor. It is due to not high enough spatial frequency used in the calculations: the distance between sampling points is too big and many important features are lost. For correct propagation/magnification the TEM_{20,0} mode use either smaller scale (e.g. $L_0 = 0.64$ cm, $N = 256$) or larger discretization ($N=512$, $L_0 = 1.28$). Try this.

Example 04. Diffraction of an Elliptical Beam

This example is given to show how sensitive the diffraction is to the shape of the beam. It demonstrates also that the aspect ratio (ellipticity) of the beam as small as 0.999 can be detected. User can reproduce these results with a Flat-topped beam (file *EXM 03-Ellipt.pls*) that has the next parameters: points = 512; scale 1.28 cm; beam size (diameter) = 0.8 cm; ellipticity = 0.99; rotation angle 60 degree; softening = 0.003 cm; wavelength 1066.7 nm.

Results of the elliptical beam propagation at the distance 120 cm *EXM 03-Ellipt.scm* are given in the next figure with various magnifications. Pictures are contrasted using Range Selection Controls (on the right side of the Beam Window). The asymmetry in the center of the picture could be detected visually in the case of ellipticity 0.99.

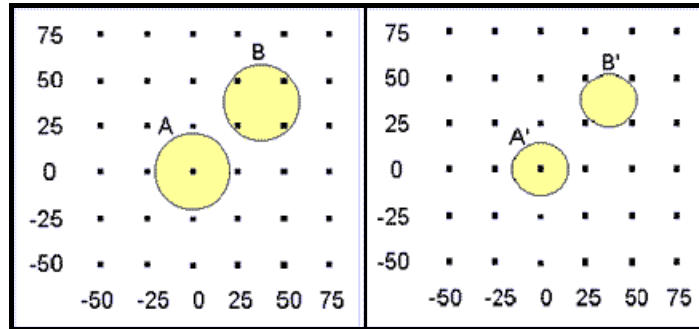


Such a small ellipticity as 0.999 could be detected also. You can reproduce this result editing the input beam parameters (changing the aspect ratio and setting rotation angle equal to 0). In this case, the asymmetry could be seen when two profile cuts are taken along X- and Y-axes through the center of the diffraction pattern.

Example 05. Obscuration

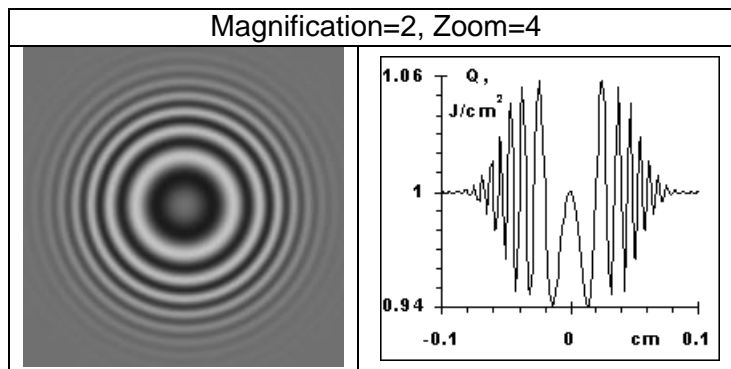
Even if you are cleaning surfaces of the optics of your installation consisting of many elements, some small size dust particles are left. The element "obscuration" is intended for their modeling as well as to model other absorbing inclusions.

Load the scheme *EXM 05-Obскур.scm* and the input beam *EXM 05-Obскур.pls*. Inspecting the beam parameters one can see that the circular beam (wavelength 2000 nm) of the diameter 0.6 cm with very soft boundary (softening 0.06 cm) was chosen. Such a softening was taken deliberately to neglect diffraction on the beam boundaries at used propagation distance.



Step of the calculation grid (distance between sampling points) is $\Delta x = 0.0025$ cm. On the way of the beam a dust particle (absorbing disk) of the diameter 0.004 cm with the center at $x=0$, $y=0$ is placed (see left figure, position A). The target, in other words the plane where the interference of the plane wave of the main beam with the spherical wave of diffraction on the dust particle is observed, is at distance 2 cm.

After propagation and magnification set Zoom=4. For contrasting of the 2D picture change Current Max and Min levels to 1.1 and 0.9 J/cm² respectively. It is possible on the profile to define positions of the maxima and minima and their values. Left figure below shows what you can see. Right figure shows the beam intensity profile taken through the center of the diffraction pattern.



After examination, change position of the obscuration center in the scheme to the new one ($x=0.00375$ cm, $y=0.00375$ cm; see left figure, position B). If in the position A the obstacle was masking only one sampling point, now it is masking four of them. Nevertheless, performing the calculations anew, one can see that the interference pattern has not changed. Obviously, its center is moved in accordance with the change of the dust particle center position.

The displacement of the dust particle center (along X and Y) for $1.5\Delta x$ was made deliberately as for twofold (and more) magnification it is possible to check the intensity for the points situated at the same distances from the obscuration center and to compare them with the previous case (A). One can see that they are identical.

It is recommended now to decrease the obscuration size down to 0.003 cm and to carry out the calculations for the cases A' and B' (right figure). Although in position B' the obstacle (obscuration) does not mask any sampling point the interference pattern is completely analogous to the case A', certainly, except for the displacement of the center of the interference rings.

Comparing interference patterns for the obscurations of 0.004 cm and 0.003 cm one can discover that the modulation depth is decreased approximately 1.8 times as the theory predicts.

Conclusions

- The obscurations permit to model the absorbing screens with the sizes from several Δx up to small portion of Δx . The obscuration could be located arbitrary with respect to sampling points. Independently of how many sampling points the real obscuration is masking (one, several, or even none) its modeling is precise within the angle $\pm \lambda/(4\Delta x)$ from the calculation axis.
- Calculation time for modeling is much less, than the time required for Fast Fourier Transform that permits to model easily tens or even hundreds of the dust particles.

EXAMPLES FOR BASIC

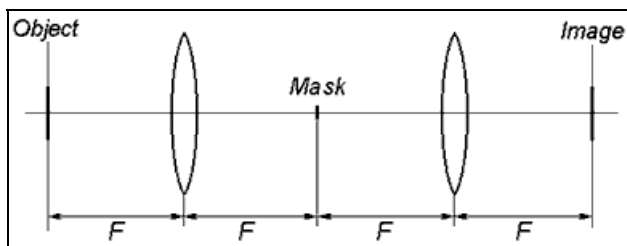
Example 10. Spatial Frequency Filtering

Spatial frequency filtering is an operation by which one removes (or passes preferentially) certain desired spatial frequencies by placing filters in the Fourier transform plane. The main kinds of filters that one encounters in the frequency filtering techniques are:

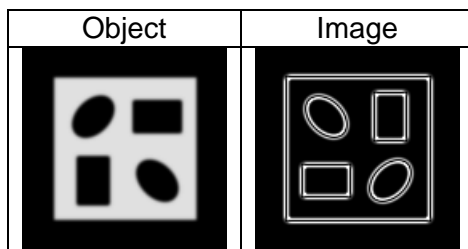
Low-Pass Filters. These filters pass only low frequencies, i.e. those frequency components lying near the axis. A typical example of their application is suppression of the high frequency beam spatial modulation using Spatial Filters in High Power Laser Systems.

High-Pass Filters. These filters allow the high frequencies pass through while the low frequencies are stopped. Such filters are used in edge enhancement.

An example of the scheme and the result of modeling are given below (results could be reproduced using *EXM 10-Contour.scm* and *EXM 10-Contour.pls*).



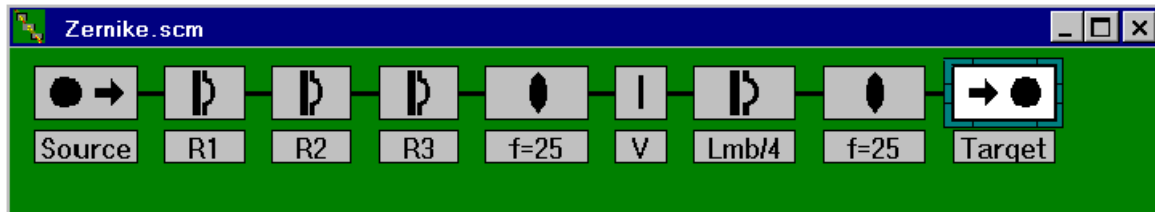
The scheme could be run with FRESNEL Demo using the discretization 128x128 sampling points that will provide the precision slightly worse than 10^{-3} . The discretization 512x512 gives the precision close to 10^{-5} .



Example 11. Zernike Phase Contrast Visualization Method

If in the optical scheme that is given in a Spatial Frequency Filtering example to replace the mask by a quarter-wave retarding plate one will get a scheme demonstrating Zernike phase contrast method. It makes possible the observation of phase objects otherwise invisible.

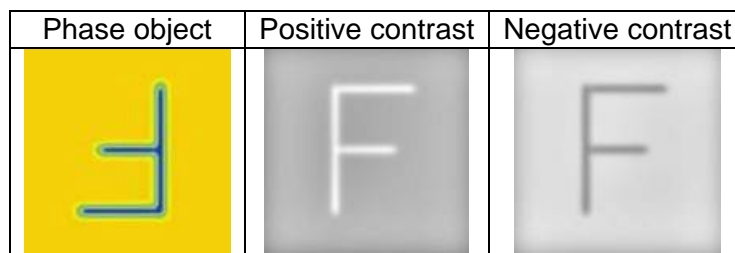
If you load *EXM 11-Zernike.scm* you will see the Scheme Window filled with elements that are required to model the operation of the Zernike method.



First three elements after Source are used to compose phase object representing the rotated letter "F". To see it:

1. Move Target to the position after R3.
2. Double click Source, choose **Load from file** | *EXM 11-Zernike.pls*.
3. Run.

When calculations are over there will be no change in the beam intensity distribution. However, if you press button  (wave front retrieval) in the Beam Window, you will get phase object in false colors "Phase object".



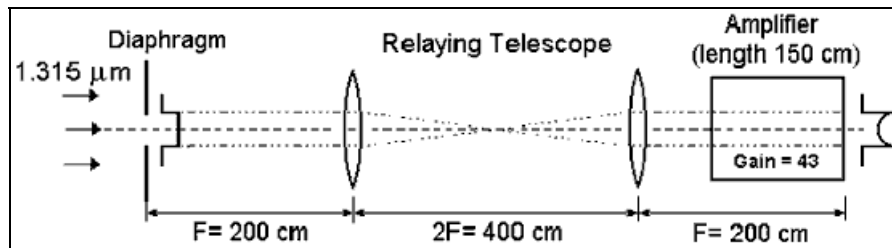
Now you can return to the initial scheme and start Run again. After finishing simulations you will see the picture labeled as "Positive contrast" (constructive interference takes place). In our case, this is for positive retardance sign of the quarter-wave plate (scheme element "Lmb/4"). Open the element dialog box and change retardance sign to negative (-0.25). When doing so, notice that the retarder is very small. It has Gaussian profile with the size $5 \cdot 10^{-3}$ cm.

When running scheme with negative retardance sign of the quarter-wave plate you will get the picture labeled as "Negative contrast" (destructive interference takes place).

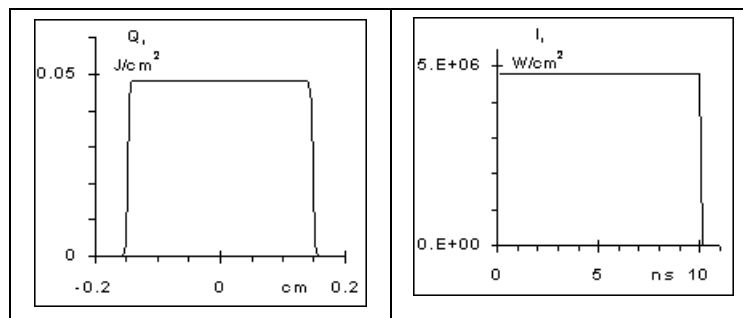
If you move the retarding plate to the position behind the Target and run the scheme, again you will see only the intensity distribution of the input beam. Pressing button  in the Beam Window, you can get image of the phase object in false colors.

Example 12. Interplay of Diffraction and Gain Saturation

The example is describing the laser beam propagation through an Iodine amplifier that exhibits nonlinear gain saturation. The scheme was taken from the paper published by Ernst E. Fill, *Optics Communications*, v.49, no.5, 362-366 (1984).



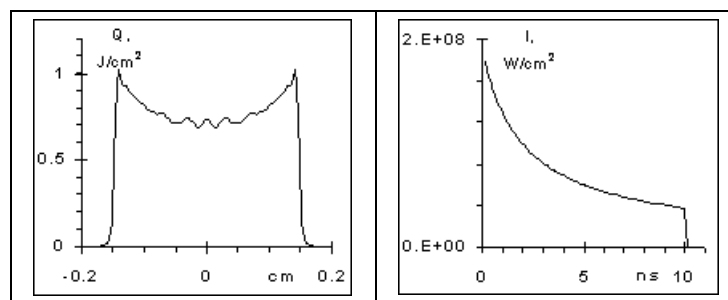
The calculations could be done using *EXM 12-Iodine.scm* and *EXM 12-Iodine.pls*. The energy density and the intensity temporal profiles right after the input diaphragm are shown in the next figure.



Parameters of Relaying Telescope and Amplifier are set according to the shown optical scheme layout. The Target was installed right at the Amplifier output (distance = 0).

The energy of the beam was selected to have the energy density at the input to the amplifier close to the saturation energy density (Q_s) for Iodine laser active medium. With high gain of the amplifier, it corresponds to strong saturation of the signal. More important is that the diaphragm size and its edge softening are chosen to provide transversal spread of the beam spatial components at the amplifier input. The Amplifier was split into 10 sections to take into account the beam transversal evolution and gain saturation along their propagation through the gain medium.

The beam spatial and temporal profiles at the amplifier output are shown in the figure below.



Note that not only the transversal beam distribution is changed due to gain saturation (on the beam edge the energy density is close to 1 J/cm^2 that is well above Q_s), but also the pulse shape is strongly deformed - the amplification of the trailing part of the pulse is much lower. Without gain or at very low input energy level the optical system gives undistorted pulse spatial and temporal profiles. Observed complex beam profile distortion occurs due to combined effect of nonlinear gain and propagation in amplifying medium that occupies Fresnel diffraction zone from $N_f=1.15$ (input to amplifier) to $N_f=inf$.

PRIMARY SEIDEL ABERRATIONS

Ideal spherical wave (wave with a plane wavefront could be regarded as having infinite radius of curvature) after traveling through a real optical system exhibits the departure from sphere that arise due to inequalities of optical path along various ray paths. The amount of departure, measured along a ray path, is known as the «Wave Aberration».

Aberrations may be specified also for any ray, which contributes to the formation of an image. If all rays starting from a given object point lie infinitesimally close to each other they form an ideal image. Those rays that make large angles to each other or travel at different distances from the optical system axis may not intersect at one point. The distance between an ideal image point and the intersection of the ray with the image plane (plane drawn through the ideal image orthogonal to the optical axis) is called «Ray Aberration».

Though the corresponding wave aberrations could be found if the ray aberrations are known, and vice versa, the wave aberrations offer a clearer physical picture. Additionally, the intensity at the given image point is best found from the wave aberrations, since these give directly the phase of the amplitude components that are taking part in formation of the image.

All types of wave aberrations could be represented as the optical path difference (OPD) across the beam cross-section $\Phi(x,y)$. Basic aberrations called also as «Primary Seidel Aberrations», include lowest order terms for dependencies of the phase versus object coordinate and ray coordinates in the pupil of the optical element. Traditionally they are represented as:

$$\begin{aligned}
 \text{Spherical aberration: } \Phi_{sph} &= -B \cdot r^4 / 4, \\
 \text{Astigmatism: } \Phi_{ast} &= -C \cdot (y_{obj})^2 \cdot r^2 \cdot \cos^2 \theta, \\
 \text{Curvature of the field (defocus): } \Phi_{def} &= -D \cdot (y_{obj})^2 \cdot r^2 / 2, \\
 \text{Distortion (tilt): } \Phi_{tilt} &= E \cdot (y_{obj})^3 \cdot r \cdot \cos \theta, \\
 \text{Coma: } \Phi_c &= F \cdot y_{obj} \cdot r^3 \cdot \cos \theta.
 \end{aligned} \tag{PA1}$$

In these expressions y_{obj} is the object coordinate in the perpendicular plane to the optical axis, $B [cm^{-3}]$, $C [cm^{-1}]$, $D [cm^{-1}]$, $E [cm^0]$, $F [cm^{-2}]$ are some constants characterizing an optical element, r, θ are polar coordinates of the ray in its pupil. The coordinate y_{obj} is dimensionless coordinate in the object plane. Quite often y_{obj} could be regarded as the inclination angle of the chief ray emanated by a source point. Terms «Defocus» and «Tilt» are often replacing traditional names «Curvature of field» and «Distortion».

Primary spherical aberration coefficients could be calculated for simple lens providing beam wave front curvature is known in the element pupil (see elements *Lens*, *Thin Lens*, and *Appendix 4*). Primary spherical aberrations for a lens or all aberrations of a tilted plane parallel plate are calculated in FRESNEL automatically for any incident beam (see *Lens A* and *Plate*).

The modeling of aberrations in FRESNEL could be accomplished using special class of elements «Primary aberrations». The magnitude of any aberration is defined by its value at the edge of the pupil equal to half of the pupil diameter $2w$. Some aberrations have an additional variable: rotation angle θ_0 (measured anticlockwise from the X -axis).

The primary wave aberrations could be rewritten in general form as

$$\Phi = A'_{lmn} \cdot \rho^n \cdot \cos^m(\theta - \theta_0). \tag{PA2}$$

Here $2l+n+m=4$ and coefficients A'_{lmn} could be expressed via *Seidel* coefficients B, C, D, E, F (see (PA4)), $\rho = r/w$. Sometimes it is convenient as well to use dimensionless number

$$K = A'_{lmn} / \lambda. \tag{PA3}$$

Supposing that the entrance and exit pupils of the optical element coincide we get:

Spherical aberration: $A'_{040} = -w^4 \cdot B/4,$

Astigmatism: $A'_{022} = -(y_{im})^2 \cdot w^2 \cdot C,$

Curvature of the field (defocus): $A'_{120} = -(y_{im})^2 \cdot w^2 \cdot D/2,$ (PA4)

Distortion (tilt): $A'_{111} = -(y_{im})^3 \cdot w \cdot E,$

Coma: $A'_{031} = -y_{im} \cdot w^3 \cdot F.$

Here y_{im} is dimensionless image coordinate corresponding to a point y_{obj} . The relations corresponding to (PA2) for various aberration types are done in the table.

Aberration type	l	n	m	Formula
Spherical	0	4	0	$A'_{040} \cdot \rho^4$
Astigmatism	0	2	2	$A'_{022} \cdot \rho^2 \cdot \cos^2(\theta - \theta_0)$
Defocus	1	2	0	$A'_{120} \cdot \rho^2$
Tilt	1	1	1	$A'_{111} \cdot \rho \cdot \cos(\theta - \theta_0)$
Coma	0	3	1	$A'_{031} \cdot \rho^3 \cdot \cos(\theta - \theta_0)$

In following sections, the aberrations are supposed to be given alternatively in nm using values of A'_{lmn} or in waves via corresponding K . Spherical aberration of a lens could be given additionally via dimensionless coefficient A_{sph} (see Appendix 4) that is connected with A'_{040} by the relation

$$A_{sph} = -A'_{040} \cdot (f/w)^4 / f. \tag{PA5}$$

Here w is the half of the lens aperture size.

All aberrations of the refractive optical elements, except for the chromatic aberration that is not discussed above, exhibit weak dependence on the wavelength. The aberrations for reflecting optics do not depend on wavelength. Therefore, the coefficients A'_{lmn} expressed in nm are more convenient for modeling of real optical systems. In this case, the variation of the wavelength by 10-20% provides high enough calculation accuracy suitable for comparison of wavelength dependent effects.

On the other hand, the aberrations expressed in waves are more convenient sometimes as far as it immediately gives an idea how big is the difference for the diffraction focus with aberrations present from the aberration-free case. The aberrations that are less than $\lambda/50$ could be ignored in most practical cases, while the aberrations of the order $(1 \div 2) \cdot \lambda$ distort the diffraction focus essentially and affect also the far field intensity distribution. Hence proper choice of the units for the aberration coefficients should be done in accordance with problem to be solved.

For circular flat-topped beams values Φ_b (nm) and K_b (waves) characterize the aberration. We shall define these values as the aberration magnitude at $r=w_b$, where w_b is the half of the beam diameter.

$$\begin{aligned} \Phi_b &= A'_{lmn} \cdot (w_b/w)^n \\ K_b &= K \cdot (w_b/w)^n \\ \Phi_b &= \lambda \cdot K_b \end{aligned} \tag{PA6}$$

As before, w is the radius of the element aperture or the normalization radius.

The focusability is one of most important characteristics for laser beams. It could be characterized by the *Strehl coefficient* that equals to the maximum intensity ratio in focal spot for the aberrated beam in comparison with that in aberration-free case

$$S \approx 1 - (2\pi/\lambda)^2 \cdot (\Delta\Phi)^2 \tag{PA7}$$

Here $(\Delta\Phi)^2 = \langle \Phi^2 \rangle - \langle \Phi \rangle^2$ is the RMS deformation of the beam wavefront.

The estimation of the maximum aberration of a beam for making the decision

Let us define the radius of the circle r_{max} with the center at $(x=0, y=0)$ and the energy outside it that is 10^{-6} of the total beam energy. Then neglecting the energy outside the circle the maximum aberration could be designated as

$$K_{max} = K \cdot (r_{max}/w)^n. \quad (PA8)$$

If K_{max} is less than the negligible aberration then this aberration is not applied. User defines the level of the negligible aberration in **Run Options**. By default, the negligible aberration is 0.01 waves.

On the other hand, too large aberration may result in the computation error. When K_{max} exceeds the permissible level of the aberration K_{lim} the warning message appears that reads, "Aberration is too high. Calculation results may be incorrect." After the warning message the program makes a pause and User can make a decision whether to continue or stop the calculations. In Example 29 the approximate formula for the permissible level of the aberrations K_{lim} is obtained. The formula is valid for all primary Seidel aberrations

$$K_{lim} = (N/n) \cdot (0.21 \cdot b + 0.02 \cdot b^2 + 0.04 \cdot b^3 - 0.27 \cdot b^4). \quad (PA9)$$

Where N is the calculation discretization, n is the power for the respective aberration dependence on ρ (see equation (PA2)), $b = 2r_{max}/L$, L is the current scale.

Two important conclusions from relation (PA9) are as follows:

- It is recommended to choose $b = 2r_{max}/L \approx 0.6 \div 0.7$ as far as K_{lim} in this case is at maximum.
- The permissible level of the aberrations is proportional to the calculation discretization.

Example 20. Spherical Aberration: Beam Focusability

Most of the laser beam transformations are accomplished using various types of lenses. For laser beams aberration both beam size $2w_b$ and the lens diameter $2w$ are important. That is why in relations given below both these parameters appear. When the beam is flat-topped and its size equals to lens diameter the relations coincide with that usually given in Optics textbooks.

The principal limitation that determines the quality of the beam during its transformations, if lenses are not tilted, is spherical aberration. According to *Marechal criterion*, the spherical aberrations of a lens could be ignored if the normalized intensity (*Strehl ratio*) in focal spot is greater or equal to 0.8. In the case of the circular flat-topped beam, the spherical aberration coefficient A'_{040} should obey the relation

$$|A'_{040}| (w_b/w)^4 = |\Phi_b| \leq 3\lambda/\pi = 0.955\lambda, \quad (EX20.1)$$

where A'_{040} (expressed in nm) corresponds to a wave aberration at radial coordinate r equal to the half of the lens diameter $2 \cdot w$, i.e. $r = w$.

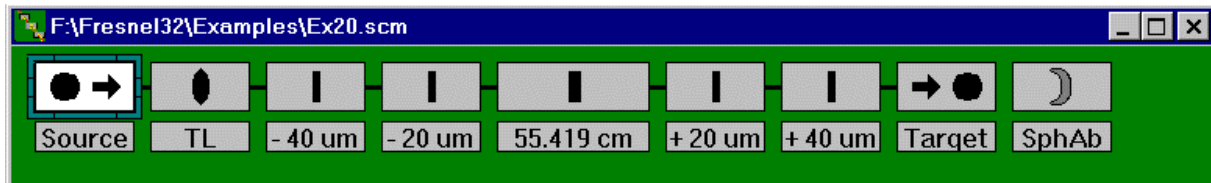
Focal spot displacement from the paraxial focus position due to spherical aberration is given by

$$\Delta Z_f = 2\Phi_b \cdot (f/w_b)^2. \quad (EX20.2)$$

For a thin lens the inequality (EX20.1) could be rewritten using (PA5) in the form

$$A_{sph} \cdot f \cdot (w_b/f)^4 \leq 0.955\lambda, \quad (EX20.3)$$

where A_{sph} is the dimensionless spherical aberration coefficient (see *Appendix 4*). For a plano-convex lens with refractive index $n=1.5$ installed in right position (plane wave hits convex surface) $A_{sph} = 0.292$. If the ratio $w_b/f = 0.05$, $\lambda = 1060 \text{ nm}$ then minimum focal length that satisfies (EX20.3) is $f \approx 55.5 \text{ cm}$ ($2w_b = 5.55 \text{ cm}$). Focal spot with maximum intensity in this case should be situated by 0.081 cm closer to the lens than paraxial focus, i.e. at the point 55.419 cm behind the lens.

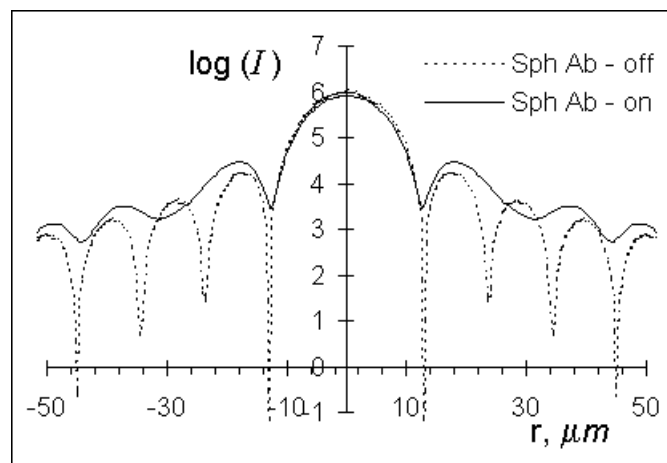


An example demonstrating operation of a lens with above parameters is given in the scheme «EXM 20.scm» (input beam is in «EXM 20.pls»). The spherical aberration could be given optionally in the *Thin lens* dialog box as $A_{sph} = 0.292$ or in *Spherical aberration* dialog box as $A'_{040} = -A_{sph} \cdot f \cdot (w_b/f)^4 \approx -1013 \text{ nm}$.

Several *View screens* are situated along the optical axis at different distances from the lens. The screen in the middle is at the plane of best focus. Other screens are 20μ and 40μ before and after the best focus plane. *Target* is in the plane of the paraxial focus that one can check by switching “off” the aberrations. In this case, the on-axis intensity at the *Target* is 10^6 J/cm^2 (use *X-profile* and *log scale* to see *Airy rings* in details). Note that the lens diameter is greater than the beam size to avoid the diffraction onto the lens aperture. Running scheme with the lens aberrations “on” one can see that the maximum intensity for the lens with aberration is 81.7 % of the intensity for aberration-free lens.

Even the spherical aberration 0.955λ results in noticeable deformation of *Airy rings* as shown in Fig where the comparison of the radial distributions for the lenses with and without aberration, respectively in the plane of best focus and the plane of paraxial focus, is presented. (To see the aberrated beam distribution with good resolution one has to move *Target* to the position right after the middle *View Screen* (55.419cm), set *Target* distance to zero, and set *Magnification* to 4^* or 8^*).

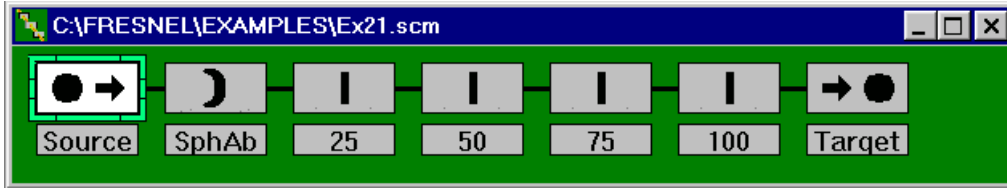
According to the equation (EX20.2) the position of the best focus plane for a lens with spherical aberrations does not depend on wavelength while the *Strehl ratio* depends on the wavelength (see Eq.(PA6), section *Primary Aberrations*). Thus if in above «EXM 20» example one changes the wavelength of the input beam to 530 or 2120 nm the result of calculations will show same position of the intensity maximum behind the lens (55.419 cm). The *Strehl ratio* will drop down to 42.8 % for 530 nm and goes up to 95.3 % for 2120 nm.



Fig

Example 21. Spherical Aberration: Beam Quality

An example of the influence of the spherical aberration onto the beam quality variation during its propagation is given in a scheme «EXM 21.scm» (input is « EXM 21.pls»).



The flat-topped beam of $2w_b = 1$ cm affected by a spherical aberration, that equals to 500 nm for $r = 0.5\text{ cm}$, propagates the distance 1 m . Despite the fact that in this case, the magnitude of the wave aberration at the beam edge is almost twice as small as in the previous example, the beam quality deterioration during propagation is dramatic as it is shown in the Fig.1. As could be seen the beam upon the propagation becomes compressed in such a way that while the intensity on the axis stays constant, the intensities at the edges are increasing. For comparison the intensity at $Z = 1\text{ m}$ is shown for the cases with (solid line) and without (dashed line) the spherical aberration. The overshoots visible on the beam edges are due to the beam diffraction.

For reasonably small spherical aberrations the relation that takes into account the wavefront slopes with respect to the beam propagation direction and describes the effect of the intensity variation with propagation distance Z is

$$I(r, Z) = I_0 \cdot (1 + 4\alpha \cdot r^2 \cdot Z)^2 / [(1 + 8\alpha \cdot r^2 \cdot Z) \cdot (1 + 16\alpha \cdot r^2 \cdot Z)] \tag{EX21.1}$$

Here $\alpha = \lambda \cdot K_b / (w_b)^4$.

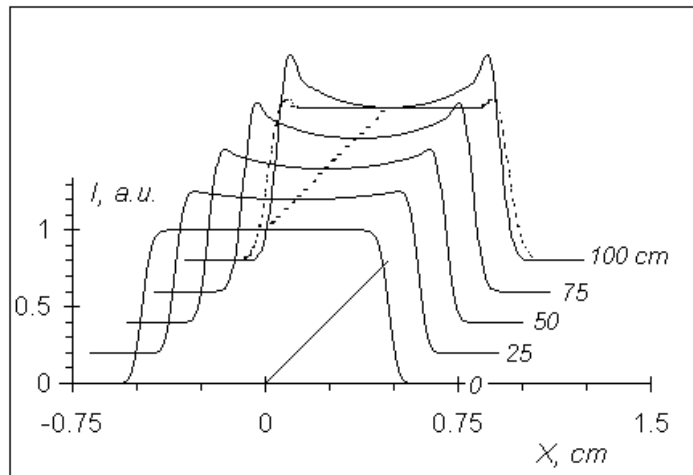


Fig.1

In this example the beam intensity variation according to (EX21.1) quite well coincides with the data of Fig.1.

The comparison of the intensity distributions with (EX21.1) at distances $Z = 75\text{ cm}$ and 100 cm is presented in Fig.2. The discrepancy present near the beam edge occurs due to the beam diffraction that is not taken into account in relation (EX21.1).

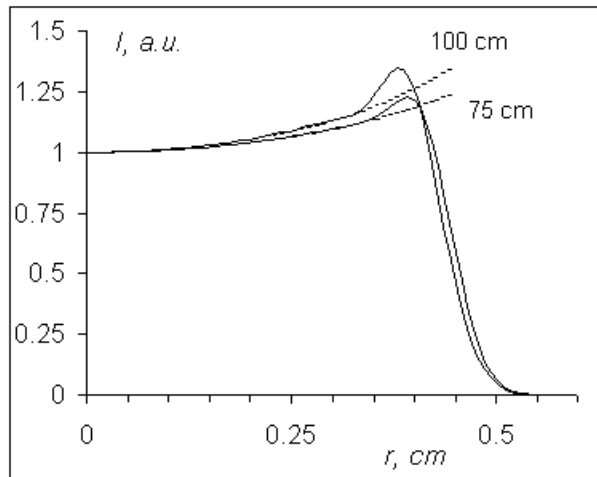


Fig.2

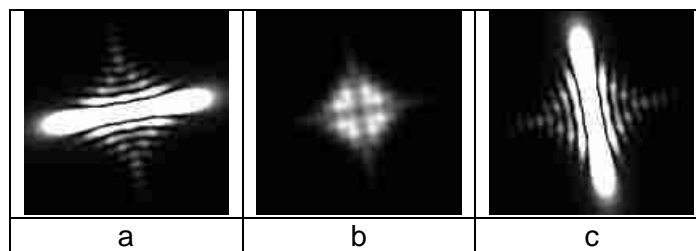
Example 22. Astigmatism

When a lens is inclined with respect to the optical axis its optical power becomes different for the rays propagating in tangential (the plane of inclination) and in sagittal planes. The effect is similar to the adding of a cylindrical lens to a normally installed conventional lens that also results in the summation of lenses power in one plane without any optical power change in another one.

The interference pattern of an unaberrated beam with an aberrated one ($K_b=5$ waves) is given below. Note that [see (PA6)] for the astigmatism $K_b=K(w_b/w)^2$.



Using the scheme *EXM 22.scm* and the beam *EXM 22.pls* ($w_b=1$ cm, $\lambda=1000$ nm) one can observe an evolution of the intensity distribution near the paraxial focus of a spherical lens. In this example: $f=10$ cm, $A'_{022}=2000$ nm = 2λ , $\theta=10^\circ$. The displacement of the sagittal focus is $Z_s=0$, while for the tangential focus $Z_t=2(f/w)^2 A'_{022}=0.04$ cm. That is why to obtain the distribution in sagittal focus (Fig. a) it is necessary to install the Target at the distance $Z=f=10$ cm. For the tangential focus (Fig. c) $Z=f+ Z_t=10.04$ cm. The distribution in the intermediate plane is given in the Fig. b. For the better visibility the images of the Figs. a and c are overexposed.



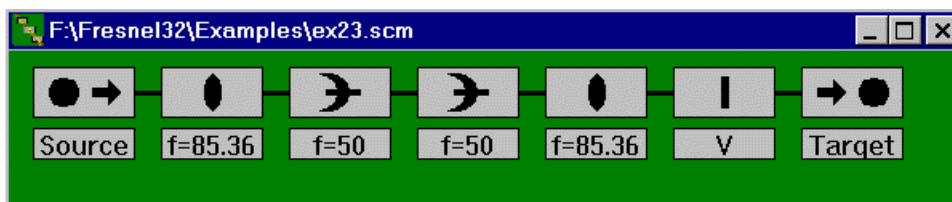
Example 23. Astigmatism: Modeling of Cylindrical Lenses.

The element *Astigmatism* could be employed to model cylindrical lenses. The relation

$$A'_{022} = -w^2/2f_c \quad (\text{EX23.1})$$

should be used to define parameters A'_{022} corresponding to an equivalent cylindrical lens with *EFL* equal to f_c and aperture $2w$. For instance for a lens with $f_c = 50$ cm, $2w = 0.5$ cm we get $A'_{022} = -6250$ nm.

An example demonstrating an optical scheme that includes both usual spherical and cylindrical lenses is shown below. This is a scheme of $\pi/2$ mode transformer that is utilized to convert *Hermite-Gaussian* (HG) modes into *Laguerre-Gaussian* (LG) modes and vice versa [LG, of a general type where an azimuthal term is given by $\exp(il \cdot \varphi)$ rather than by $\cos(l \cdot \varphi)$ or $\sin(l \cdot \varphi)$]. The theory of the mode conversion could be found in: M.W.Beijersbergen, et al., *Astigmatic laser mode converters and transfer of orbital momentum*, Optics Communications, v.96, pp.123-131 (1993).



This scheme is designed to convert the HG_{01} mode with the waist size $w_0 = 0.04146$ cm and flat phase front into the LG_{01} mode of the same size but with the phase front that is spiraling along the propagation direction as shown in the Fig.

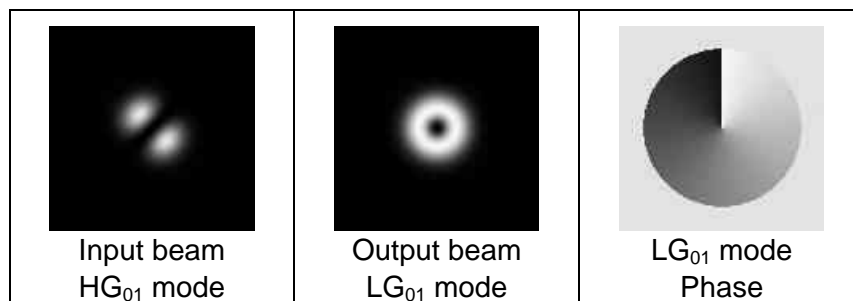


Fig.

The modes conversion could be reproduced with *EXM 23.scm* and *EXM 23.pls*.

TELESCOPES

Example 30. Beam Expander: Imaging by Keplerian and Galilean Expanders

Calculations made for this example could be reproduced using files «EXM 30.scm» ($f_1=2.5\text{cm}$, $f_2=12.5\text{ cm}$), «EXM 30a.scm» ($f_1=-2.5\text{ cm}$, $f_2=12.5\text{ cm}$) and «EXM 30.pls» for both schemes.

Keplerian Beam Expander ($f_1 > 0$, $f_2 > 0$) transforms input beam in such a way that for beam cross section (or object) situated in front of the first expander lens one can find its inverted image behind the second lens. This is possible if the object plane satisfies the relation

$$(f_1/f_2) \cdot (f_1 + f_2) \geq Z_{obj} \geq 0. \quad (\text{EX30.1})$$

The image position behind the second lens is given by

$$Z_{im} = (f_2/f_1) \cdot (f_1 + f_2) - Z_{obj}(f_2/f_1)^2. \quad (\text{EX30.2})$$

In above relations Z_{obj} is positive to the left of the first lens and $Z_{im} > 0$ to the right of the second lens. For example at $Z_{obj} = (f_1/f_2) \cdot (f_1 + f_2) = 3\text{ cm}$ we get $Z_{im} = 0$, what means that the image is situated at the plane of the second lens («EXM 30.scm»). This image reproduces all details of the object without any diffraction as shown in the Fig.1.

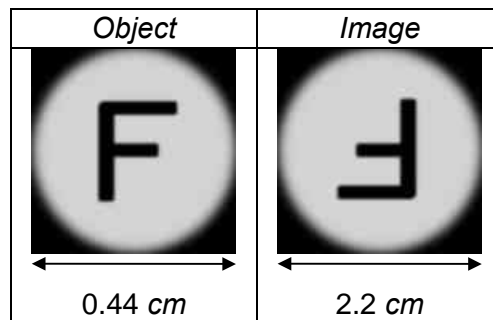


Fig.1

Galilean Beam Expander ($f_1 < 0$ or $f_2 < 0$, $f_1 + f_2 > 0$) in contrary to Keplerian one has no imaging properties. This could be seen from relation (EX30.1). There are no object planes in front of the first lens that are conjugated with corresponding image planes behind the second lens. At any $Z_{obj} \geq 0$ the image planes are at $Z_{im} < 0$.

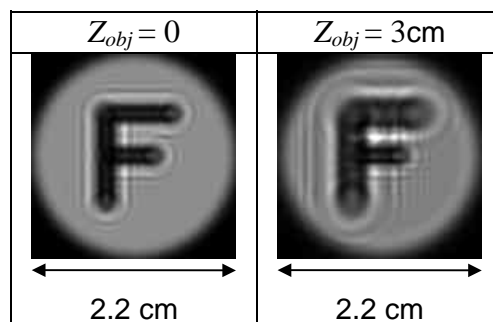


Fig.2

All images on the screen placed behind the second lens exhibit diffraction «EXM30a.scm». As could be shown, the minimum distance between the virtual image and the second lens plane is at $Z_{obj} = 0$. As could be seen in Fig.2 the diffraction pattern near the object edges in this case is less pronounced than at any $Z_{obj} > 0$.

Example 31. Beam Expander: Spherical Aberrations and Beam Quality

High quality beam expanders usually use microscope objective lens as a front lens and corrected doublet as a rear lens. Additionally, to avoid diffraction the beam should occupy only a fraction of the lens apertures. The flat-topped beam size, for example, should not be greater than 0.8 (for a Gaussian beam less 0.5) of the front lens aperture.

Typical fabrication accuracy of the lens surfaces usually is not much better than $\lambda/5$. Hence, the residual spherical aberration of the lenses should not introduce the wave aberration of the beam larger than $\lambda/5$ ($|K_b|=0.2$). This means that if one takes a flat-topped beam with the size 0.8 of the front lens aperture, the total retardance that is set in Beam Expander dialog box should obey the inequality

$$|\Phi| < 0.2 \cdot \lambda \cdot (w_l/w_b)^4 = 0.2 \cdot \lambda \cdot (1.25)^4 \approx 0.5 \cdot \lambda, \quad (\text{EX31.1})$$

where w_b and w_l are respectively the half of the beam size and the half of the beam expander front lens aperture.

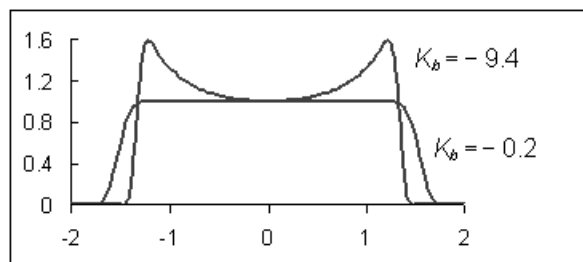
The retardance -0.5λ is the default value set in the dialog box of the Beam Expander (see « *EXM 31.scm* »). At this value of the aberration a beam with the size matching the above limitation ($0.8w_l$, «*EXM 31.pls*») being expanded up to the diameter 3.2 cm will propagate for several meters without essential deterioration. Even at $Z=5$ m the beam is flat to within 2%. The flat-top beam deterioration due to spherical aberration is described by equation (EX21.1) (see section *Spherical Aberration*) that for this case could be reduced to

$$I(r=w_b) \approx I_0 (1 - 16 \cdot K_b \cdot Z/Z_R), \quad (\text{EX31.2})$$

where Z is the propagation distance after the Beam Expander and $Z_R = w_b^2/\lambda$ is the *Rayleigh distance* of the beam.

Being inverted (used to compress the beam, «*EXM 31a.scm*» and «*EXM 31a.pls*»), above Beam Expander will have the same retardance $K_b = -0.5$ at the edge of the aperture of the lens with shorter focal length. The propagation without the beam deterioration after the beam expander in this case, of course, is much shorter as soon as *Rayleigh distance* of the compressed beam is 256 times shorter than in previous scheme «*EXM 31.scm*».

A similar beam expander consisting of uncorrected plano-convex (or plano-concave and plano-convex) lenses with small F -numbers («*EXM31b.scm*», «*EXM 31.pls*») exhibits a very poor quality. The comparison of the output beam distributions at the distance 2 m behind the beam expander for schemes «*EXM 31.scm*» ($K_b = -0.2$) and «*EXM 31b.scm*» ($A_{sph} = 0.292$, equivalent $K_b = -9.4$) is given in the Fig.



Uncorrected lenses could be used only at large $F\#$. For a beam expander with $M=16$ that expands the flat-topped beam of 0.2 cm size one should use lenses with focal lengths 3.6 and 57.6 cm and $F\# \approx 14$. Only in this case the quality of the beam expander consisting of uncorrected plano-convex (or plano-concave and plano-convex) lenses will be satisfactory.

BEAM TRANSFORMS

It is accepted that beam transforms operations do not change the polarization of light.

Shift is the beam movement in XY plane with no changing beam propagation direction. This operation can model such ordinary experimental situations as:

- Propagation through tilted plate,
- Reflection from two parallel mirrors.

Beam shift is especially necessary for modeling the situation when the elements of optical systems have the same optical axis before and after beam movement.

Rotation is the beam turn around Z-axis ($x_0 = y_0 = 0$) in XY plane. This operation can model such schemes as:

- Dove prisms,
- General case for reflection from two mirrors,
- Using of beam rotation may be useful when optical axes before and after some element(s) have no intersection in space.

It is possible to rotate a beam relatively to an axis (x_0, y_0) that is parallel to Z-axis. To do this some one have to use both **Rotation** and **Shift** options in FRESNEL.

When using **Rotation** and **Tilt** elements, a turn of the beam around an axis, which is not parallel to Z-axis, takes place.

Reflection is an operation that is similar to mirror image. It has mathematical designation as inversion relatively the plane. In FRESNEL, it is supposed for simple reflection operation that inversion plane includes Z-axis.

In optical experiments, the mirrors are used quite often. Some times, it is convenient to represent the beam the way as you see it after reflection. This is modeled with **Reflection** transform.

Applying **Shift** and **Reflection**, it is possible to make inversion relatively the plane, which is parallel to Z-axis and is located at some distance from Z-axis.

Inversion relatively the plane that is not parallel to Z-axis may be modeled with help of **Tilt** and **Reflection**.

To simulate beam transforms operations Fast Fourier Transform (FFT) is used in FRESNEL. This technique gives usually very precise results. Therefore the values as small as 10^{-5} of grid pixel size for **Shift** and 10^{-7} degree for **Rotation** can be visualized. To do this someone may use **Interference** element for destructive interference.

EXAMPLE 40. Beam Shift: Accuracy, Simulation Noise

First, we denote displacement in polar and Cartesian coordinates:

Polar: r_{sh} – shift value, θ_{sh} – shift direction angle,

Cartesian: x_{sh} – shift in X-direction, y_{sh} – shift in Y-direction.

Obviously that $x_{sh} = r_{sh} \cdot \cos\theta_{sh}$ and $y_{sh} = r_{sh} \cdot \sin\theta_{sh}$.

Displacement can be represented as operator or formula.

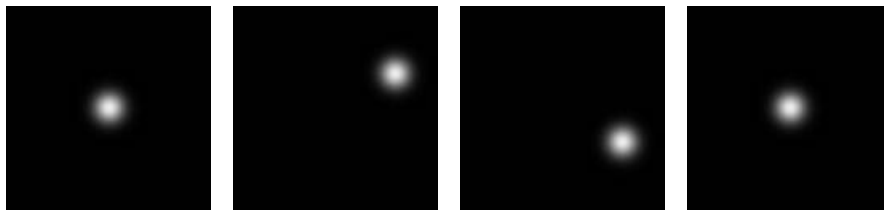
$$A_{out}(x, y) = [SH(x_{sh}, y_{sh})] * A_{in}(x, y) \quad \text{or} \quad A_{out}(x, y) = A_{in}(x - x_{sh}, y - y_{sh}) \quad (\text{EX40.1})$$

Beam displacement can be specified by a user and is simulated with accuracy **better** than calculation **grid step**. To check it choose the scheme EXM 40 .scm, which represents the shift at the distance $r_{sh} = 0.5$ cm in the direction $\theta = 30^\circ$. The final position of the beam center (centroid) does not coincide with a sample point of calculation grid for both X- and Y-axes. Running the scheme with EXM 40 .pls one can see shifting the beam to a predefined position with accuracy of 10^{-7} . To check it please uses the *Beam Analyzer* – a feature of FRESNEL. You can compare:

$x_c = 0.4330127$ cm that equal $r_{sh} \cdot \cos(30^\circ)$ and $y_c = 0.25$ cm that equal $r_{sh} \cdot \sin(30^\circ)$.

Next realization (EXM 40a .scm and EXM 40. pls) refers to calculation precision or in the other words demonstrates simulation noise for *Beam Shift* operation.

The scheme represents three displacements ($r_{sh} = 0.5$ cm, $\theta_1 = 30^\circ$, $\theta_2 = -90^\circ$, $\theta_3 = 150^\circ$), which result in returning the beam (EXM 40. pls) to its initial position. It is shown in the pictures.



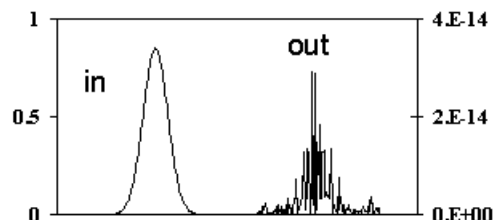
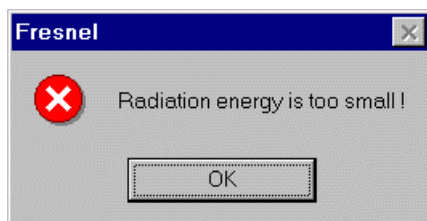
Applying the formula (EX40.1) three times, we have:

$$A_3(x, y) = [SH_3] * [SH_2] * [SH_1] * A_{in}(x, y) = A_{in}(x, y).$$

As soon as $\cos(30^\circ) + \cos(-90^\circ) + \cos(150^\circ) = 0$ and $\sin(30^\circ) + \sin(-90^\circ) + \sin(150^\circ) = 0$.

Therefore, the resulting beam should be the same as the initial one.

Load (EXM 40. pls) beam as the BEAM 2 in the *Interference* element. In this case, the superposition of the beam after three displacements and of the initial beam delayed at 0.5 waves will take place. After passing *Interference* element the warning message will appear, which means that the total current energy is less than 10^6 photons.



The X-plots before and after superposition are shown on the right. Pay attention that on the plot **In** and **Out** flux scales are quite different! **Comparison** of the plots of **In** and **Out** beams shows that resulted field amplitude (flux square root) is only 10^{-7} of input amplitude. This value gives relative precision or simulation noise for *Beam Shift* operation.

EXAMPLE 41. Beam Shift: Acceptable values.

The shift is too small.

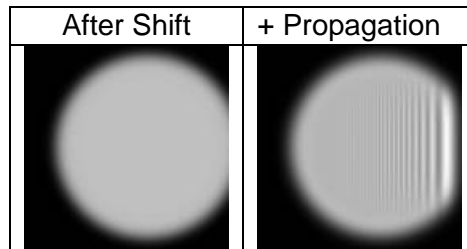
Code **does not apply shift operation** if absolute values of both x_{sh} and y_{sh} are less than $10^{-5} \cdot L_0 / N$, where L_0 is waist size for calculation grid and N is discretization. Note that $L_0 \leq L_c$ (L_c is the current scale) and might be much less. Both values (L_0 and L_c) can be seen in the Table of Beam and Grid Parameters.

The shift is too big.

On the other hand, some displacements can be unreasonably high for modeling.

For User convenience FRESNEL estimates acceptable displacement and invokes warning message when necessary. The warning message reads, "*Shift is large. Calculation results may be incorrect*". This estimation takes a place when *Precision check* is *on* in *Run options* dialog box.

In some cases the problem is evident which happens when a part of a beam will be out of the current calculation scale. This is demonstrated in the example (EXM41 .scm by using EXM41 .pls). The result after a shift one can see on the left picture – only a small part of the beam is out of the current scale. The right one shows pseudo - diffraction fringes, which appear on the next simulation step (propagation at 55 cm) due to computation error (aliasing effect).



In order to obtain a correct result place the "*Grid control*" element before the "Shift" - this will increase the scale from 3 cm up to 4 cm.

The other situation may be not so evident at first sight. If the shift is much less, than the current scale but it is close or exceeds half of the waist size for calculation grid this may be the problem. This is shown in the next example (EXM41a .scm and EXM41a .pls). You have a pause to compare the desired shift ($y_{sh} = -0.3$ cm) with $L_c = 10.24$ cm – OK and with half of the waist size for calculation grid ($L_0 / 2 = 0.25$ cm) – real problem. The problem occurs because the absolute value of the Y-shift is larger than $L_0 / 2$. The table shows the calculation results.

Z (m)	0	0.5	1.0	1.5	2.0	4.0
X-shift (cm), N=256	0.1	0.1	0.1	0.1	0.1	0.1
Y-shift (cm), N=256	-0.3	-0.175	-0.05	0.075	0.2	0.7
Y-shift (cm), N=512	-0.3	-0.3	-0.3	-0.3	-0.3	-0.3

After propagations, Y-shift of the beam (third row) does not correspond to the expected one. Beam direction has changed also. As in the previous example "*Grid control*" is very useful. Drag it to the place just after the "*Source*" element. Now one must increase the number of grid points. It does help - see the fourth row. Such improvement occurs due to increased number of grid points that correspondingly leads to increasing of the grid waist. After the lens for $N=512$ half of the waist size for calculation grid is 0.5 cm that bigger than shift $|-0.3|$ cm.

EXAMPLE 42. Beam Rotation: Accuracy, Simulation Noise

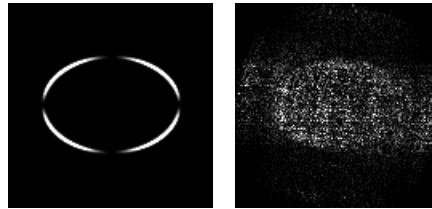
Turn of a beam around Z-axis could be represented as operator or formula.

$$A_{out}(r, \theta) = [RT(\theta_{rot})] * A_{in}(r, \theta) \quad \text{or} \quad A_{out}(r, \theta) = A_{in}(r, \theta - \theta_{rot}), \quad (\text{EX42.1})$$

θ_{rot} is a rotation angle.

Accuracy of the beam (EXM 42 .pls) rotation can be tested by simulation EXM 42 .scm. In that example, a beam turns three times for the angles (21° , -15° and -6.998°). The *Beam Analyzer* shows the output beam orientation (azimuth) 0.0020017° that differs from the ideal case by $1.7 \cdot 10^{-6}$ deg, which is much better than any practical measurement method of image (beam) orientation.

Possibilities of visualization of a very small rotation and of the calculation noise are demonstrated in the next example. Before running the following scheme (EXM 42a .scm) load the beam (EXM 42 .pls) as a BEAM 2 into the *Interference* element. Pay attention that the retardation between the beams is 0.5 waves, which means that destructive interference will take place. The input beam is the same EXM 42 .pls. Three rotations result in the beam turn only by one arc second. Nevertheless, such a small difference of orientations can be clearly seen on the left picture.



This picture is demonstrating the sensitivity of destructive interference method for visualization of very small beam movements. Almost the same method can be used to monitor changes of beam size or position.

Correct a rotation angle in the third element to the exact value -7° , which will result in identical orientation of the beam after three rotations and of the input one. Now the interference of the beams will demonstrate just simulation noise. You can see typical noise picture on the right figure.

The noise flux (J/cm^2) gives information about standard deviation of amplitude (A) due to calculation precision. One can deduce the following formula:

$$\text{rms}(A)/A = (2 \cdot Q_{noise}/Q_{in})^{0.5}. \quad (\text{EX42.1})$$

This expression is valid for almost constant input amplitude. Here Q_{noise} is flux of the noise and Q_{in} is the input beam flux.

After substitution the results of calculation (Q_{noise} and Q_{in}) for corrected EXM 42a .scm we have that relative simulation noise is equal to $3 \cdot 10^{-7}$.

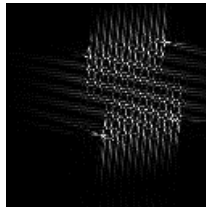
EXAMPLE 43. Beam Rotation: Errors caused by abrupt boundary

The fundamental calculation error for Fast Fourier Transform (FFT) is an aliasing effect due to abrupt boundaries. In other words it happens when calculation grid step (pixel size Δx) is not small enough to describe the boundary smoothing function.

In FRESNEL Complementary error function (Erfc) is used for boundary softening. This function gives good simulation results when amplitude softening length (δ) is more than $2 \cdot \Delta x$ and noticeable error for δ is less than $0.5 \cdot \Delta x$.

As soon as FFT is used to simulate the rotation, aliasing effect can take place. This can be demonstrated by using EXM 43 .scm and EXM 43 .pls where a mask blocks a part of the beam. The mask boundary softening is $\delta = 0.5 \cdot \Delta x = 0.005$ cm.

First you must save the beam **after the mask** and load it as BEAM 2 in the *Interference* element of the scheme EXM 43 .scm (retardance between the beams must be set to be 0.5 waves). During the simulation *Precision Warning* message will appear. Then after three rotations and destructive interference, you can see a 2D distribution of the simulation errors. The result is demonstrated in the figure.



In the picture shown is only a central part of the calculation grid where the biggest errors occur. The image is "overexposed" in sake of better visualization. Quantitative analysis shows that the mean absolute value of amplitude error is $3 \cdot 10^{-3}$ and its maximum is $1.7 \cdot 10^{-2}$.

To avoid this kind of error one has to make softening length at least twice more than the step of the calculation grid. It can be done by different ways:

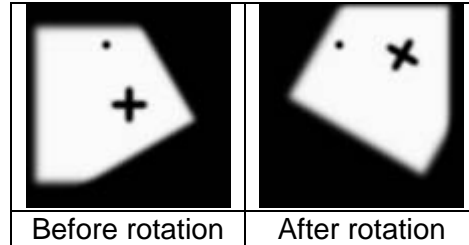
- Increasing four times the softening length if possible or
- Increasing four times the discretization (N) or
- Increasing two times the softening length and two times the discretization.

If you do this, the simulation accuracy will be of the order of 10^{-7} . The test picture will look almost the same as the right picture of the previous (42) example.

EXAMPLE 44. Beam Rotation: Arbitrary Center of Turn

Rotation of the beam relatively to an arbitrary center having coordinates (x_0, y_0) is possible using both *Shift* and *Rotation* transforms. This means that the beam rotation is performed relatively to an axis that is parallel to Z-axis.

In the figure, you can see the beam rotation around the center marked by a black point. Before rotation, the cross on the beam coincides with the grid origin (left picture).



Such a rotation may be shown using EXM 44 .pls and any of the schemes: EXM 44a .scm, EXM 44b .scm, or EXM 44c .scm.

To simplify the formulas below, we denote the rotation centre in cylindrical coordinates (r_0, θ_0) . Angle of rotation is θ_{rot} . For this example it was chosen that $r_0 = 0.4$ cm; $\theta_0 = 111^\circ$; $\theta_{rot} = 60^\circ$.

Method A (EXM 44a .scm):

1. **Shift** at the value r_0 in the direction $(\theta_0 - 180^\circ)$,
2. **Rotation** at the angle θ_{rot} ,
3. **Shift** at the value r_0 in the direction (θ_0) .

Method B (EXM 44b .scm):

1. **Rotation** at the angle θ_{rot} ,
2. **Shift** at the value $2r_0 \cdot |\sin(\theta_{rot}/2)|$ in the direction $(\theta_0 - \varepsilon \cdot 90^\circ + \theta_{rot}/2)$.

Here $\varepsilon = \text{sign}(\sin \theta_{rot})$.

Method C (EXM 44c .scm):

1. **Shift** at the value $2r_0 \cdot |\sin(\theta_{rot}/2)|$ in the direction $(\theta_0 - \varepsilon \cdot 90^\circ - \theta_{rot}/2)$,
2. **Rotation** at the angle θ_{rot} .

Here $\varepsilon = \text{sign}(\sin \theta_{rot})$

Using Methods B or C it is possible to turn the beam (if the angle is not too big) around the centre, which lies outside of the calculation grid. The limitation on the angle is due to a limitation for *Shift* operation (see example 41).

Using **Rotation** and **Tilt** elements one can rotate the beam around an axis that is not parallel to Z-axis. If you will come across any problems in it's modeling, please contact FRESNEL software team.

Conclusion - it is possible to rotate a beam (radiation) relatively almost any axis until an aliasing effect happens.

EXAMPLE 45. Beam Reflection: Two Reflections equal Rotation

Reflection (inversion) of a beam relatively to the plane $y = tg(\theta_{inv}) \cdot x$ can be represented as operator or formula.

$$A_{out}(r, \theta) = [RFL(\theta_{inv})] * A_{in}(r, \theta) \quad \text{or} \quad A_{out}(r, \theta) = A_{in}(r, 2 \cdot \theta_{inv} - \theta), \quad (EX45.1)$$

θ_{inv} is an angle between the inversion plane and X-axis.

Applying twice formula (EX45.1) we have after two reflections

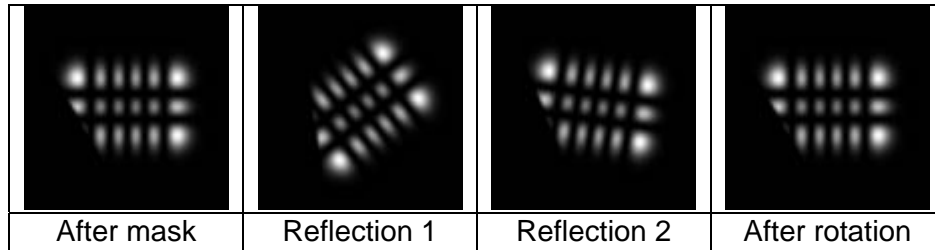
$$A_{out}(r, \theta) = A_{in}(r, \theta - 2 \cdot (\theta_2 - \theta_1)). \quad (EX45.2)$$

Comparing formulas (EX45.2) and (EX42.1) we obtain $\theta_{rot} = 2(\theta_2 - \theta_1)$. Here θ_1 is the angle of inversion axis for the first reflection and θ_2 for the second.

To check this use EXM 45 .scm that consists of:

1. Input radiation (EXM 45 .pls), which is TEM_{5,2} HG mode,
2. Mask to make beam asymmetrical,
3. Reflection 1 with the angle of inversion plane $\theta_1 = 19^\circ$,
4. Reflection 2 with the angle of inversion plane $\theta_2 = 15^\circ$,
5. Rotation at the angle 8° .

Gradually beam images are shown in the figure below.



To inspect EX45.2 quantitatively compare azimuth values in *Beam Analyzer* after the mask and after rotation. You will find that they are equal.

For estimation of the simulation noise of the *Reflection* transform, you may use destructive interference as it was done in EXAMPLE 42 (EXM 42a .scm). It will show that the noise is approximately 10^{-7} .

Applying **Shift** and **Reflection** it is possible to make inversion relatively the plane, which is parallel to Z-axis and is located at some distance from it.

Inversion relatively the plane that is not parallel to Z-axis may be modeled with the help of **Tilt** and **Reflection**.

OBSTACLES II

Foreign inclusions in glass, dust particles, the scratches and so on cause intensity fluctuations due to diffraction effect. In most cases, it is the main reason for the intensity noise in laser beams (speckle pattern). Modulation depth can be big enough even when size of particles and total occupied area is much less than beam size and area. The correct simulation of the modulation value and spatial frequencies is important for modeling nonlinear optical effects.

Obscuration is an element that is introduced to model very small obstacles like specks, dust particles on optical surfaces, etc. The obscuration is treated as completely opaque. The values of intensity fluctuations and suppression of the fluctuations by spatial filter are discussed in Examples 60, 63. The accuracy of obscurations modeling is demonstrated on the base of Babinet's principle in Examples 61, 62.

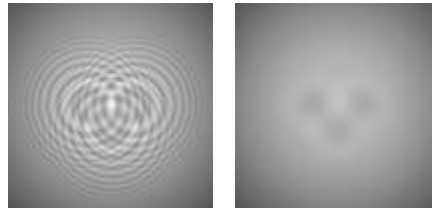
Dusty surface means transparent optical surface with the specks of dust that is left on it. User defines an area (aperture) and number of specks. The specks will be placed randomly and their positions will change from one simulation to another. When **fix specks position** option will be chosen then the specks location will be the same in the different simulations. Diffraction on many of specks leads to perturbation of beam – see Example 64. Far field distribution and ability of spatial filtering are discussed in Examples 65, 66.

EXAMPLE 60. Obscuration: Three Small Specks, Spatial Filtering

In this example is demonstrated the result of a superposition (interference) of waves diffracted on the specks and initial beam.

The input radiation is a Gaussian beam (EXM 60 .pls) with a size of 0.5 cm and of 500 nm wavelength. For this beam, the length of the waist is almost 40 meters. Three circle obscurations are placed in the beam way (EXM 60 .scm). Each has a diameter of 30 microns and they are displaced 180 microns from the beam center correspondingly to the left, right and upwards. The losses due to absorption on specks is $2.14 \cdot 10^{-4}$ of input energy.

Disturbed beam travels the distance of 4.5 cm. Resulting distribution is shown below (left).



The magnification 8^* is used on the Target for better observation of the central part of the beam. The maximal intensity spike exceeds initial level by 18%. Pay attention that the propagation distance of 4.5 cm is 100 times greater than the Rayleigh distance for these obscurations. You can delete some of the specks or add new ones to see how it will change the interference pattern.

Is it possible to decrease the depth of intensity modulation or in the other words to improve beam distribution for further applications? Yes, it is when the size of obscuration(s) is much smaller than the beam size. **Spatial Filter** can do it.

Two **rules** must be followed to realize spatial filtering successfully:

1. Pinhole size has to be big enough in order not to disturb the beam.
2. Pinhole size has to be as small as possible for the best suppression of intensity modulation caused by specks.

We will postpone calculation of the pinhole optimal size for next examples. Here we will try to optimize it in simulation experiment.

Move now **Spatial Filter** element (EXM 60 .scm) to the position after the obscurations. This Spatial Filter consists of identical lenses with focal length of 100 cm. Change target distance to 200 cm (plane 1) which will correspond to the image plane of the specks, or to 204.5 cm (plane 2) which will correspond to the distance of 4.5 cm after the image plane of the specks. Choose both in successive simulations to compare results.

For different pinhole sizes, you will have:

- Pinhole is 1 cm. In plane 1 separated speck images are resolved; the valley depths are 40%. Central spike decreased slightly to 14.5% in plane 2.
- Pinhole is 0.5 cm. In plane 1 separated speck images still are resolved; the valley depths are 12%. Peak to valley difference is equal to 8% in plane 2. See the **right picture**.
- Pinhole is 0.25 cm. Both in plane 1 and plane 2, speck images are not resolved any more; amplitude departure from a Gaussian distribution is 1.2%.
- Pinhole is 1 mm. In both planes amplitude departure from a Gaussian beam is 0.6%.
- **Pinhole is 0.4 mm**. Probably it is the best pinhole size. Amplitude departure from a Gaussian distribution is 0.11%.
- Pinhole is 0.2 mm. Amplitude departure from a Gaussian distribution is 8%. Total energy of the beam decreased 0.8% (energy losses).

Further decreasing of a pinhole size will cause greater and greater Gaussian beam disturbance and its energy losses. This contradicts to the above-mentioned rule #1.

EXAMPLES 61 and 62. Obscuration: Babinet's principle

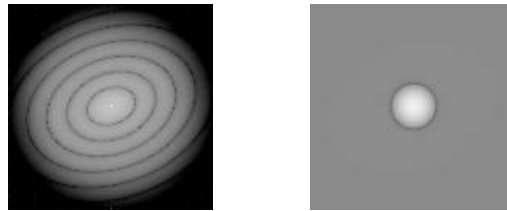
Babinet's Principle states that opaque objects (mask, obscuration) produce the same diffraction patterns as their complementary holes. It can be written as:

$$A_1(\text{obs}) + A_2(\text{hole}) = A_0 \quad (\text{EX61.1})$$

Here A_0 is the field incident to an obstacle, A_1 is the field after an obstacle and A_2 is the field after the complementary hole. Sometimes it is convenient to represent (EX61.1) as

$$A_1(\text{obs}) = A_0 - A_2(\text{hole}) \quad (\text{EX61.1a})$$

Babinet's Principle can be used to test the validity of an obscuration modeling. In the scheme (EXM 61 .scm) an elliptical obscuration is placed on the way of the beam (EXM 61 .pls). Far field distribution of the diffraction pattern is shown on the left picture.



Far field intensity of the Gaussian beam (central bright point) exceeds speck's diffraction intensity 7 orders of magnitude. Therefore, overexposed logarithmical scale has to be used for visualization of the speck's diffraction pattern. In FRESNEL, one can check that dark and bright elliptical rings correspond to diffraction pattern of the complementary elliptical hole according to expression (EX61.1a).

The right picture represents the central part of the left one with resolution 32 times better. A dark ring (almost of zero intensity) is clearly seen. As it follows from the right part of expression (EX61.1a) it has to take place in the points where absolute values of A_0 and A_2 are equal. This dark ring diameter is of about an optimal pinhole size for spatial filtering. Such kind of a picture can be used for "experimental" choice of a pinhole size.

The **Example 62** relates to accuracy testing of **obscuration modeling**. One can do it with the help of Babinet's Principle.

Rectangular beam (EXM 62 .pls) is disturbed by a speck and propagates 6 centimeters (EXM 62a .scm). This corresponds to the left part of expression (EX61.1a). Note that speck size includes only 8 calculation pixels (sample points). Therefore, modeling accuracy has to be tested.

Right part of the expression (EX61.1a) is represented by (EXM 62b .scm). A small part of the beam passes through the diaphragm (complementary hole) and propagates the same distance (6 cm). Just after the diaphragm, more than a thousand of sample points correspond to the size of the hole. This happens due to auto magnification procedure in FRESNEL. The diffraction wave (A_2) is calculated with a good precision. **The resulting field of superposition takes place after Interference element.** When you compare X - plots of the two simulations you will see a good agreement.

The FRESNEL procedure responsible for modeling of very small obscurations, describes diffraction for angles less than $0.4 \cdot \lambda / \Delta x$ very precisely and good enough for angles that are less than $0.6 \cdot \lambda / \Delta x$. This means, that if in a simulated optical setup there exists some diaphragm (aperture of element, pinhole) limiting such angles, modeling will be very exact.

EXAMPLE 63. Obscuration: Pinhole size optimization

The optimum size of a pinhole in a spatial filter is determined by the following limitations:

1. Pinhole size has to be big enough in order not to disturb the main beam.
2. Pinhole size has to be as small as possible for the best suppression of intensity modulation caused by specks.

Let us denote Gaussian beam size $d = 2 \cdot w$ and its size in the pinhole plane of a spatial filter as $d_f = 2 \cdot w_f$. They are connected according to the expression:

$$d_f = 4 \cdot \lambda \cdot f / (\pi \cdot d) \quad (\text{EX63.1})$$

Here f is the focal length of the spatial filter first lens.

For the input beam (EXM 63a .pls) its wavelength is $\lambda = 0.5 \mu$ and $d = 0.5$ cm. Optical setup in (EXM 63a .scm) represents a half of a spatial filter with its first lens focal length of $f = 100$ cm. A pinhole is placed in the rear focal plane of the lens. Before a pinhole, the beam is Gaussian and its size d_f equals to 0.0127 cm. For a Gaussian beam, the ratio of the intensity $J(r)$ at a point r to the intensity J_0 at beam center and corresponding amplitude A ratio equal to

$$J(r) / J_0 = \exp[-2 \cdot (r/w_f)^2] \quad (\text{EX63.2})$$

$$A(r) / A_0 = \exp[-(r/w_f)^2] = \varepsilon \quad (\text{EX63.3})$$

For pinhole size $d_{pin} = 0.02$ cm, intensity at its boundary can be calculated using (EX63.2). Substituting $r = 0.01$ cm we have $J(r) / J_0 = 7.2 \cdot 10^{-3}$. The same value gives energy losses for a Gaussian beam that passed through the pinhole. The result of diffraction is shown at Fig 1. The left plot corresponds to the distance of 0.4 cm, while the right – to 0.5 cm behind the pinhole.

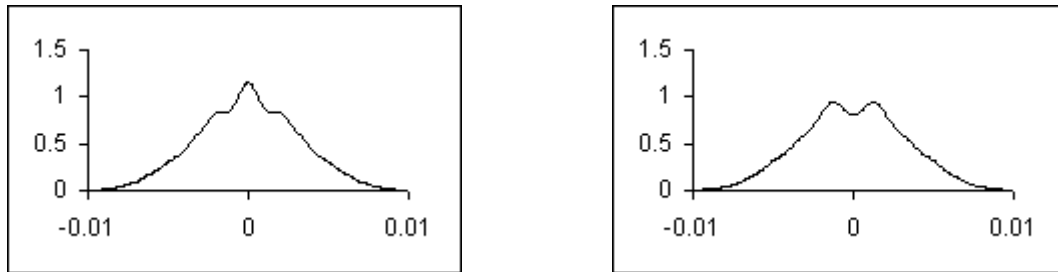


Fig 1

They both differ from Gaussian distribution. Maximal deviation is 17%. The intensity deviation at the center (Dev) for diffracted Gaussian beam can be calculated as

$$Dev = (1 \pm \varepsilon)^2 - 1 \approx 2\varepsilon \quad (\text{EX63.4})$$

Substitution from (EX63.3) $\varepsilon = 8.5 \cdot 10^{-2}$ ($r = 0.01$ cm) to (EX63.4) gives deviation at center 0.17 or 17%. Such beam deformation is not acceptable especially when some nonlinear effects may take place. If in (EXM 63a .scm) you increase now the pinhole size to the value of $d_{pin} = 0.04$ cm you will see that the beam is almost Gaussian at any propagation distance. From above formulas maximal deviation for $r = 0.02$ cm is 10^{-4} . Therefore, when a pinhole size exceeds Gaussian beam size in the pinhole plane **three times**, probably this satisfies most of applications. For high power laser the exceeding should be even more.

Will introduce the value μ according $d_{pin} = \mu \cdot d_f$. This value means that the pinhole size is μ times over the Gaussian beam size in the pinhole plane. Then modulation depth after spatial filtering can be written as

$$A_{sp} / A_0 = \mu^2 \cdot (d_{sp} / d)^2 \text{ and } A_{sp} / A_0 = 9 \cdot (d_{sp} / d)^2 \text{ for } \mu = 3 \quad (\text{EX63.5})$$

- A_0 is amplitude of the Gaussian beam after spatial filter (no speck);
- A_{sp} is amplitude of speck diffraction wave that is left after spatial filter;

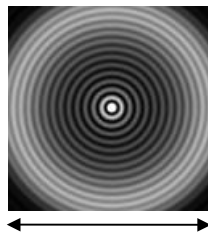
- d is input Gaussian beam size;
- d_{sp} is speck size.

Expression (EX63.5) shows that effective spatial filtering takes place when speck size is much smaller than Gaussian beam size. This can be verified using (EXM 63 .scm) and (EXM 63 .pls). Starting speck size $d_{sp} = 0.2 \cdot d$ is very big in comparison with the beam. It hardly can be called a “speck” for this particular beam. Decreasing the speck size, you can check fitness with the expression (EX63.5).

Modeling of speck diffraction wave.

Expression (EX63.4) gives deviation at the center of beam only. Someone who is interested in the effect in more details can use (EXM 63b .scm). This scheme is the same as the scheme (EXM 63a .scm) but a complementary mask (with the same size) replaces the pinhole. Input beam (EXM 63b .pls) is the same as (EXM 63a .pls) but it is given at quite a different scale - 100 cm. This was done for better **resolution** in the mask plane in order to **minimize** the simulation **errors**. (Using the Grid Control element with an output scale of about 2 cm for the beam (EXM 63b .pls), you will see that this one and beam (EXM 63a .pls) are identical). There is a pause just after the mask to observe the light that is left behind it. Note that the ring you will see after the mask is a part of a Gaussian beam, which was blocked by the pinhole.

Fig 2 shows a 2D diffraction pattern of the ring at a distance of 0.4 cm. In order to clearly see the outer diffraction rings, adjust *Max current range* to the level of 0.002.



0.025 cm

Fig 2

This is one of the possible realizations of the Poisson's bright spot for a Gaussian beam, which also has another name – the Spot of Arago.

The left part of Fig 3 presents a radial plot of amplitude for this distribution.

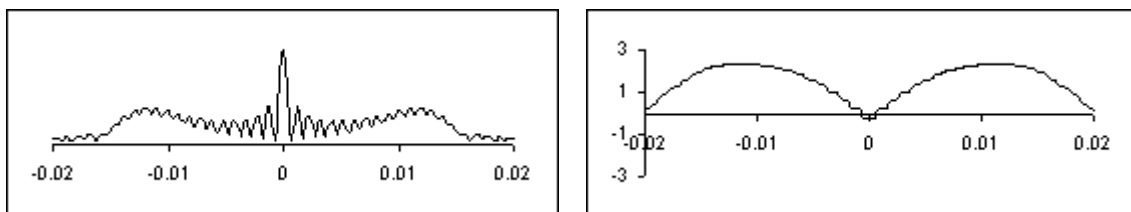


Fig 3

The right one gives the phase front where the scale of ordinate axis is in waves.

Superposition of this field with an undisturbed Gaussian beam leads to the distribution shown on figure 1.

EXAMPLE 64. Dusty surface (Dust): Noise - intensity fluctuation

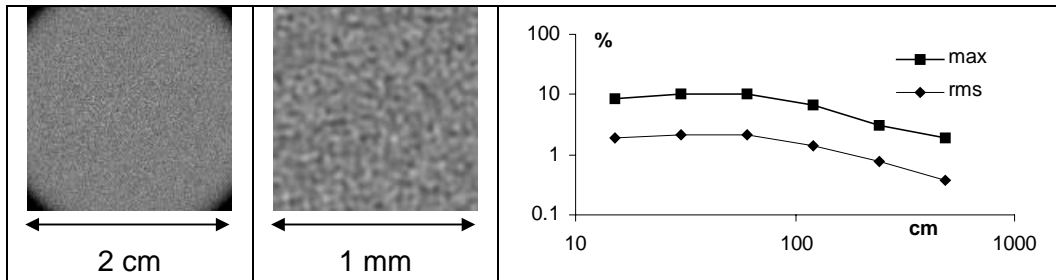
As soon as specks are placed randomly, their number in the beam area will change from one realization to another. According to statistical laws, relative uncertainty is equal to $1/m^{0.5}$, where m is a mean number of specks in the beam area. Energy dissipation l_{ss} due to absorption on specks can be written as

$$l_{ss} = m_0 \cdot S_{sp} / S_{ap} \cong m \cdot S_{sp} / S_{beam}, \text{ where } m = m_0 \cdot S_{beam} / S_{ap} \quad (\text{EX64.1})$$

Here m_0 is a total number of specks defined by the User, S_{ap} is an aperture area of a dust element, S_{sp} is a speck area and S_{beam} is the area of the beam. We will name value l_{ss} as “**net losses**”. In a real optical setup there may exist other losses in case when an aperture (pinhole) cuts off a part of diffraction wave from a speck.

The influence of a dusty surface on the beam (EXM 64 .pls) is demonstrated in the scheme (EXM 64 .scm). Approximately 400 specks disturb the beam that has 3 cm diameter. The speck diameter is 30 microns and, therefore net losses equal to $4 \cdot 10^{-4}$. Certainly, after propagation for some distance, intensity distribution will be disturbed by diffraction waves from many of the specks.

The left picture represents almost the whole beam at the distance 60 cm after a dusted surface. The other one is a central part of the same distribution with much better resolution. We will describe how to obtain this picture. Drag *Grid control* element to the position after the element that has the name “Z=60 cm”. *Grid control* has the following new grid parameters: Points equals 256; Scale is 0.1 cm. If you change the Scale to 2 cm, you will obtain the left picture. At the distance of 60 cm, maximal intensity exceeds the mean intensity by 10%, and fluctuation size equals approximately 50 microns. Both values vary as a function of distance from dust. When you will run the initial scheme (EXM 64 .scm) you will see the dependence.



The plots show the dependences of Max fluctuation of intensity and of standard deviation (rms) of intensity fluctuations as a function of distance z from dusted surface. Relations (EX64.3) and (EX64.2) describe the dependences of Max intensity and standard deviation of fluctuations.

$$Rms = (l_{ss})^{0.5} \text{ for } z < z_1 \text{ and } Rms = (l_{ss})^{0.5} \cdot (z_1/z) \text{ for } z > z_1 \quad (\text{EX64.2})$$

$$Max = 5 \div 6 \cdot Rms \quad (\text{EX64.3})$$

Here $z_1 \cong d \cdot d_{sp} / \lambda$; d and d_{sp} are beam and speck diameters.

It is useful to keep in mind some limitations for correct modeling of the dust. To minimize overlapping of modeling functions for neighbored obscurations (specks) the net losses have to be confined (EX64.4).

$$l_{ss} < 0.05 \cdot (k/k+6)^2 \text{ for } k \leq 10; \quad l_{ss} < 0.05 \cdot (k/k+2)^2 \text{ for } k > 10, \quad k = d_{sp} / \Delta x \quad (\text{EX64.4})$$

FRESNEL has the option that is randomly changing speck's position from one simulation to the other. It is clear that most of results (net losses, maximal and standard deviation of intensity) will not be reproducible when the mean number of specks m in the beam is not too big. This gives limitation for minimal losses:

$$l_{ss} \cong m \cdot (L^2 / S_{beam}) \cdot (k/N)^2 \text{ or } l_{ss} > 300 \cdot (k/N)^2 \text{ for } m > 100, \quad (L^2 / S_{beam}) = 3 \quad (\text{EX64.5})$$

Here L is the current scale. Division (EX64.4) by (EX64.5) gives that for $N \geq 2048$ we have some freedom for modeling different experimental situations.

EXAMPLE 65. Dust: Far field diffraction

Net losses (l_{ss}) determine a part of beam area that is stopped by dust. Such losses decrease amplitude of incident wave in Fraunhofer zone.

$$A_d = A_0 \cdot (1 - l_{ss}) \quad (\text{EX65.1})$$

Here A_d and A_0 are far field amplitudes for presence and absence of dust. Correspondingly, for intensity we have

$$I_d = I_0 \cdot (1 - l_{ss})^2 \cong I_0 \cdot (1 - 2 \cdot l_{ss}) \quad (\text{EX65.2})$$

This is a well-known effect that far field intensity of incident wave is decreased twice more compared with absorption losses. For absorbing obstacles, scattering (diffraction) losses are equal to absorbing losses in accordance with Babinet's Principle. This is probably the simplest explanation of the effect. More rigorous proof one can find in optical textbooks.

Optical setup EXM 65 .scm demonstrates the above conclusion. When there is no dust, far field flux for the input beam EXM 65 .pls is 1 J/cm . You will check it if you drag the **Dust** element behind the Target and make a simulation. Net losses are equal to 1% (open dialog window to see it). Simulation with the **Dust** element "on" shows far field flux to be 0.98 J/cm^2 according to (EX65.2).

Far field diffraction for an individual speck was discussed in Example 61. Diffraction for many identical obscurations gives (see left picture) the same distribution **on average** as for one obscuration. To reproduce this result you can use EXM 65a .scm and EXM 65 .pls. The left picture corresponds to elliptical shape of specks. If you will change the shape of the specks to rectangular ones, the scattered light will be like the distribution presented on the right picture. Certainly, the total diffracted energy is proportional to the number of specks in the beam area. Intensity is given in logarithmical scale on both pictures of Fig 1.

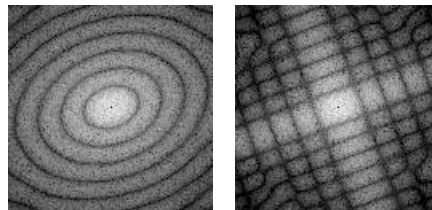


Fig 1

Careful investigation shows that for a big number of specks far field distribution of diffracted light consists of randomly placed small spots. To see it with better resolution you should change the output grid scale in *Grid control* element (e.g. to 0.625 cm). The result is shown on Fig 2. Now you see only a small part of diffracted light lying close to propagation direction of the incident beam.

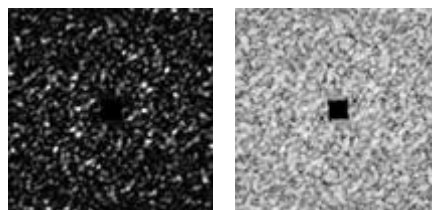


Fig 2

The intensity scale is linear for the left picture and it is logarithmical for the right one. Black square (no light) in the center of both pictures corresponds to the mask placed in the back focal point of the lens. The mask size is $0.5 \times 0.5 \text{ mm}^2$. Such method (mask) is commonly used in experiments for blanking high intensity main beam. This allows seeing the weak scattered (diffracted) light otherwise invisible.

EXAMPLE 66. Dust: Spatial filtering of intensity noise

Examples 60 and 63 demonstrated spatial filtering efficiency for intensity modulation caused by individual specks. Present example shows that for lots of specks in the beam area spatial filtering is efficient also.

The results you can reproduce with EXM 66 .scm and input beam EXM 66 .pls. *Dust* element has 5060 specks randomly placed inside a 2.1 cm-aperture square. Each speck is a circle with a diameter of 20μ . These numbers define net losses to be $3.6 \cdot 10^{-3}$. Only some part of the specks (approximately 230) occurs in a circle with a diameter of 0.5 cm.

Parameters of the beam and of the spatial filter are the same as in examples 60 and 63. Therefore optimal pinhole size equals to 0.4 mm (see corresponding formulas). The front lens of the spatial filter is placed at a distance of 7 cm after the *Dust* element. The images of this plane after spatial filter as well as the plots are shown on the figures below. 2 D pictures represent only a small central part ($1.3 \cdot 1.3 \text{ mm}^2$) of the beam while the plots show almost the whole beam.

In the case when pinhole is absent, maximal amplitude departure from the ideal Gaussian beam equals to 16%.

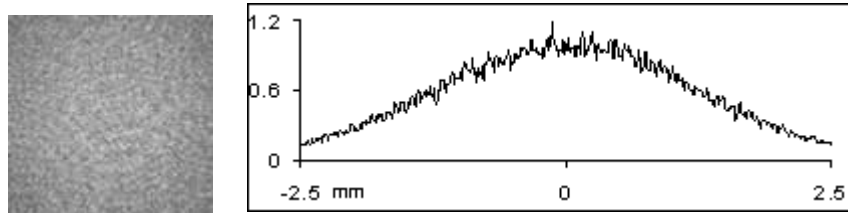


Fig 1 - no spatial filtering

Diffraction angle for the specks is 0.03 rad. Therefore, spatial filtering already takes place for a pinhole size of 1 cm ($f=100 \text{ cm}$) – noise spatial frequency and intensity fluctuations are decreased. Amplitude departure from Gaussian distribution is 6% (Fig 2).

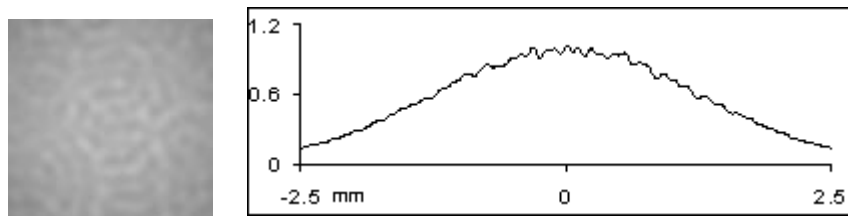


Fig 2 – pinhole size is 10 mm

For optimal pinhole size 0.4 mm the beam is very close to Gaussian. The maximal amplitude departure is less than 0.1%.

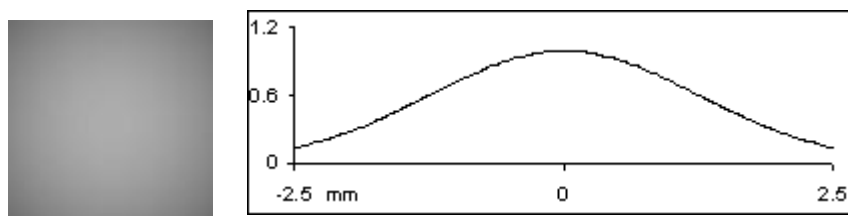


Fig 3 - pinhole size is 0.4 mm

The *Spatial filter* cut off diffraction waves from specks. This leads to total attenuation of the output beam by a factor $(1-2 \cdot I_{ss})$ – see example 65. Therefore a reference beam to be used for comparison has to be an input one multiplied by a factor $(1-2 \cdot 3.6 \cdot 10^{-3}) = 0.9928$. Such a beam after propagation of 7 cm serves as an ideal beam for comparison.